iScience

CellPress
OPEN ACCESS

Article

Cannabinoid receptor type 1 (CB_1R) inhibits hypothalamic leptin signaling via β-arrestin1 in complex with TC-PTP and STAT3

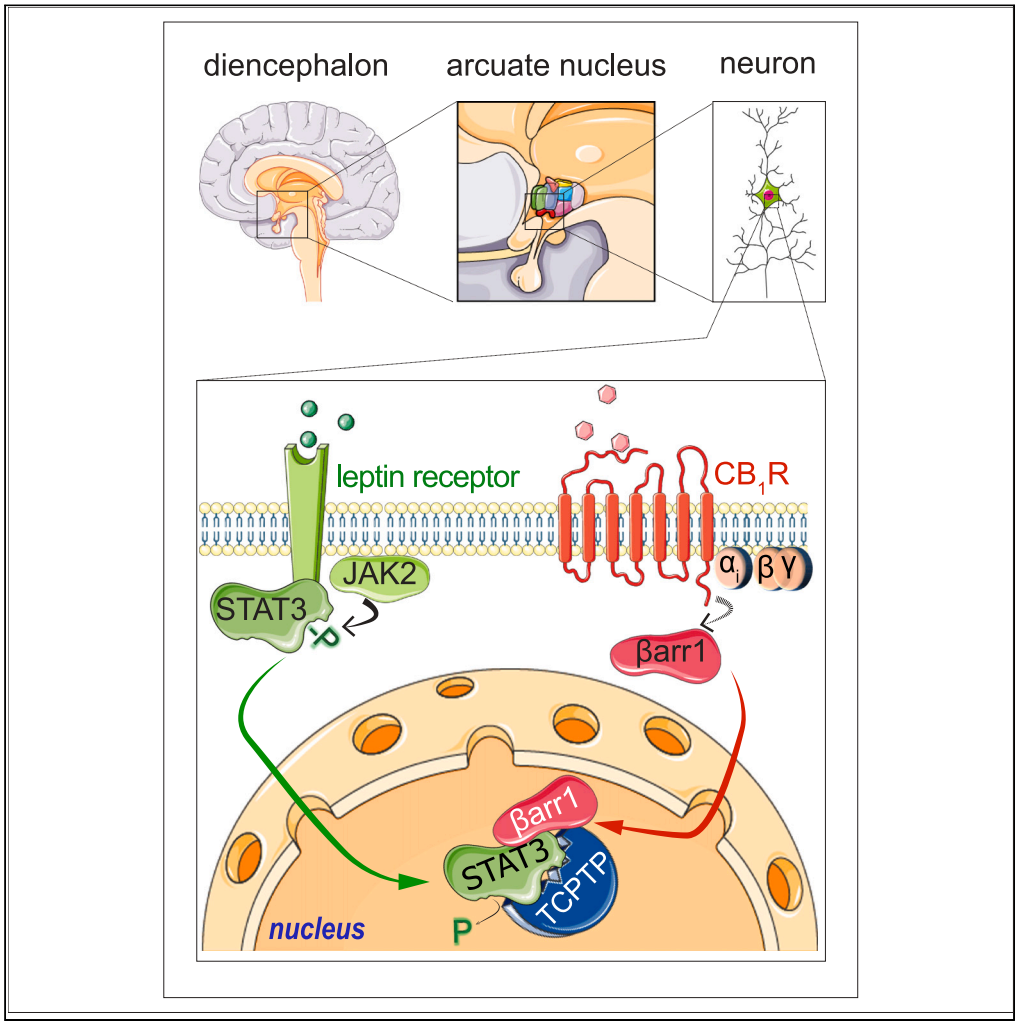

Gergő Szanda, Tony Jourdan, Éva Wisniewski, ..., András Spät, Joseph Tam, George Kunos

szanda.gergo@med.semmelweis-univ.hu (G.S.)
george.kunos@nih.gov (G.K.)

Highlights

Leptin-induced STAT3 phosphorylation is attenuated by CB_1 receptor agonists

Upon CB_1 and leptin receptor co-stimulation β-arrestin1 translocates to the nucleus

β-arrestin1 binds STAT3 and the nuclear phosphotyrosine phosphatase TC-PTP

TC-PTP then dephosphorylates STAT3

Szanda et al., iScience 26, 107207
July 21, 2023
https://doi.org/10.1016/j.isci.2023.107207

iScience

CellPress
OPEN ACCESS

Article

Cannabinoid receptor type 1 (CB_1R) inhibits hypothalamic leptin signaling via β-arrestin1 in complex with TC-PTP and STAT3

Gergő Szanda,[1,8,9,*] Tony Jourdan,[2] Éva Wisniewski,[1] Resat Cinar,[3] Grzegorz Godlewski,[3] Anikó Rajki,[1,8] Jie Liu,[3] Lee Chedester,[3] Bence Szalai,[1] András Dávid Tóth,[1,4] Eszter Soltész-Katona,[1,5] László Hunyady,[1,5] Asuka Inoue,[6] Viktória Bea Horváth,[1] András Spät,[1] Joseph Tam,[7] and George Kunos[3,*]

SUMMARY

Molecular interactions between anorexigenic leptin and orexigenic endocannabinoids, although of great metabolic significance, are not well understood. We report here that hypothalamic STAT3 signaling in mice, initiated by physiological elevations of leptin, is diminished by agonists of the cannabinoid receptor 1 (CB_1R). Measurement of STAT3 activation by semi-automated confocal microscopy in cultured neurons revealed that this CB_1R-mediated inhibition requires both T cell protein tyrosine phosphatase (TC-PTP) and β-arrestin1 but is independent of changes in cAMP. Moreover, β-arrestin1 translocates to the nucleus upon CB_1R activation and binds both STAT3 and TC-PTP. Consistently, CB_1R activation failed to suppress leptin signaling in β-arrestin1 knockout mice *in vivo*, and in neural cells deficient in CB_1R, β-arrestin1 or TC-PTP. Altogether, CB_1R activation engages β-arrestin1 to coordinate the TC-PTP-mediated inhibition of the leptin-evoked neuronal STAT3 response. This mechanism may restrict the anorexigenic effects of leptin when hypothalamic endocannabinoid levels rise, as during fasting or in diet-induced obesity.

INTRODUCTION

The combination of palatable food and sedentary lifestyle destabilize the balance between anabolic and catabolic processes eventually culminating in body weight increase.[1] Obesity and its corollaries pose a global health threat[2] and, despite the considerable progress in our understanding of energy metabolism on the molecular level, treatment options in obesity are still disturbingly limited,[3] and effective therapies often have serious side effects.[4] This necessitates further exploration of the mechanisms that regulate energy homeostasis.

Leptin and endocannabinoids play central and generally opposing roles in the control of energy metabolism. Adipocyte-derived leptin reduces food intake and increases energy expenditure via pleiotropic actions in the hypothalamus and brainstem.[5,6] Diminished sensitivity to leptin, referred to as leptin resistance, is a hallmark of obesity,[7] and alleviating hyperleptinemia and leptin resistance is sufficient to reduce food intake and body weight in diet-induced obesity.[8] By contrast, the endocannabinoid system, comprising the type-1 and type-2 cannabinoid receptors (CB_1R and CB_2R, respectively) and their endogenous ligands anandamide and 2-arachidonoylglycerol,[9] generally favors positive energy balance via both central[10,11] and peripheral CB_1Rs.[12] Their importance in energy metabolism is well illustrated by the observations that these receptors are essential for the development of leptin resistance and diet-induced obesity[13] and that CB_1R blockade readily alleviates obesity and its corollaries.[14,15]

There exists a multi-layered interaction between leptin and endocannabinoids. Leptin rapidly decreases the concentration of endocannabinoids specifically in the hypothalamus[16,17]; and this effect likely enhances leptin's catabolic potential.[18] Leptin also supresses the CB_1R-dependent stimulation of orexigenic melanin-concentrating hormone (MCH) neurons[19] and, in diet-induced obesity, that of orexin neurons.[20] On the other hand, genetic ablation of CB_1R in the ventromedial hypothalamus (VMN) was shown to increase sensitivity to a pharmacological dose of leptin,[21] and CB_1Rs may interfere with leptin-induced

[1]Department of Physiology, Semmelweis University Medical School, 1094 Budapest, Hungary

[2]INSERM Center Lipids, Nutrition, Cancer LNC U1231, 21000 Dijon, France

[3]Laboratory of Physiologic Studies, National Institute on Alcohol Abuse and Alcoholism, National Institutes of Health, Bethesda, MD 20892, USA

[4]Department of Internal Medicine and Haematology, Semmelweis University, 1085 Budapest, Hungary

[5]Institute of Enzymology, Research Centre for Natural Sciences, Centre of Excellence of the Hungarian Academy of Sciences, 1117 Budapest, Hungary

[6]Graduate School of Pharmaceutical Sciences, Tohoku University, Sendai 980-8578, Japan

[7]Obesity and Metabolism Laboratory, The Institute for Drug Research, School of Pharmacy, Faculty of Medicine, The Hebrew University of Jerusalem, Jerusalem 9112102, Israel

[8]ELKH-SE Laboratory of Molecular Physiology Research Group, Eötvös Loránd Research Network, 1094 Budapest, Hungary

[9]lead contact

*Correspondence: szanda.gergo@med.semmelweis-univ.hu (G.S.), george.kunos@nih.gov (G.K.)

https://doi.org/10.1016/j.isci.2023.107207

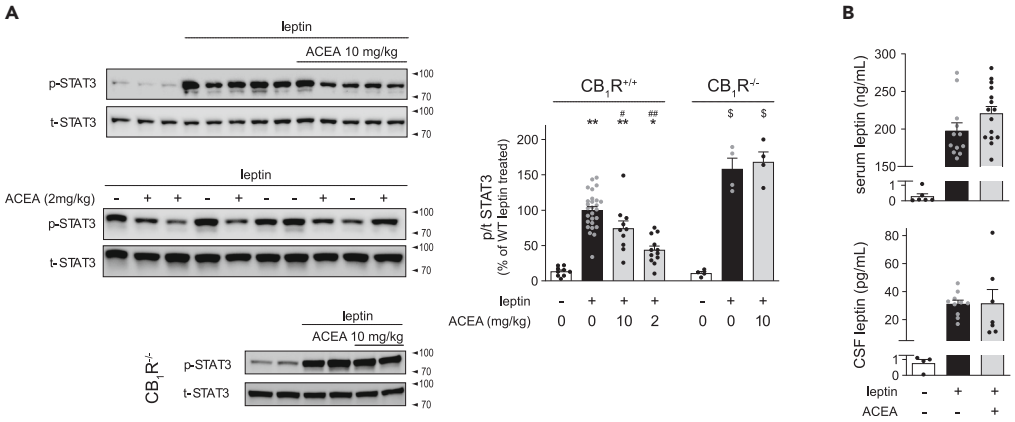

Figure 1. Cannabinoids dampen leptin-induced STAT3 phosphorylation in the mediobasal hypothalamus

(A) Western blot measurement of exogenous leptin-induced hypothalamic STAT3 phosphorylation in the presence or absence of CB_1R agonist. Overnight fasted 12-16-week-old wild type ($CB_1R^{+/+}$) or CB_1R (*cnr1*) knock out ($CB_1R^{-/-}$) mice were treated with ACEA (10 or 2 mg/kg; *i.p.*) or vehicle 30 or 45 min prior to leptin (0.3 mg/kg, *i.p.*) or saline treatment. The mediobasal hypothalamus was removed 45 or 60 min after leptin injection and STAT3 phosphorylation was assessed by western blotting. Number of observations for the bar graph from left to right (L to R): n = 9–27-12-10-4-4-4; $^{**}p < 0.001$ and $^{*}p = 0.033$ when compared to WT leptin$^-$/ACEA$^-$, $^{\#\#}p < 0.002$ and $^{\#}p = 0.029$ vs. WT leptin$^+$/ACEA$^-$, $^{\$}p < 0.0001$ vs. $CB_1R^{-/-}$ leptin$^-$/ACEA$^-$ (ANOVA and Sidak's *post-hoc* test).

(B) Plasma (upper panel) and cerebrospinal fluid (CSF, lower panel) concentration of leptin in animals treated with leptin (0.3 mg/kg) or saline in the absence or presence of ACEA (2 mg/kg). Animals were fasted and treated as described for *Panel A*. Upper panel: n = 6–12-15 (L to R); $^{*}p < 0.02$ vs. ACEA$^-$/leptin$^-$ (ANOVA and Kruskal-Wallis *post-hoc* test). Lower panel: n = 4–10-7 (L to R, from 2 independent experiments); $^{*}p < 0.05$ vs. ACEA$^-$/leptin$^-$ (ANOVA and Kruskal-Wallis *post-hoc* test). (See also Figure S1).

Mean + S.E.M. are shown.

reactive oxygen species production.[22] However, the exact molecular pathways conveying these effects are not fully elucidated and the possibility of a direct inhibition of leptin signaling by cannabinoids has not yet been tested. We report here that, in fact, a transient increase in CB_1R activity blunts physiological leptin signaling in the mediobasal hypothalamus *in vivo*, and also *in vitro* in cultured neurons that lack complex synaptic connections. We show that CB_1Rs recruit the T cell protein tyrosine phosphatase (TC-PTP) in a β-arrestin1 dependent manner to inhibit one of the main intracellular effectors of leptin, STAT3. This mechanism will blunt hypothalamic leptin signaling when (endo) cannabinoid availability is high.

RESULTS

Cannabinoids dampen leptin-induced STAT3 phosphorylation in the mediobasal hypothalamus

To test whether central leptin sensitivity may be acutely modulated by cannabinoids, we assessed hypothalamic leptin signaling in the presence or absence of a CB_1R agonist by measuring STAT3 tyrosine phosphorylation (Y705), which is a sensitive and selective readout of leptin receptor signaling.[23] Overnight fasted lean male mice were treated with a moderate pharmacological dose of mouse recombinant leptin (0.3 mg/kg, *i.p.*) with or without pre-treatment with the CB_1R selective anandamide analogue arachidonyl-2′-chloroethylamide (ACEA[24]). CB_1R activation decreased leptin-evoked STAT3 tyrosine phosphorylation in the mediobasal hypothalamus (Figure 1A) and this inhibition was absent in CB_1R knockout mice (Figure 1A and S1A). The synthetic cannabinoid CP 55,940 had a similar effect (Figure S1B).

Importantly, CB_1R activation did not affect plasma and liquor leptin concentrations (Figure 1B) and had no significant effect on the hypothalamic expression of the long isoform *Lepr* (leptin receptor, long isoform [ObR_b]) or that of *Socs-3*, a classic endogenous inhibitor of STAT3-signaling[25] (Figure S1C). Moreover, the inhibition of leptin signaling by CB_1Rs was not secondary to tetrad effects as 2 mg/kg ACEA readily attenuated the hypothalamic STAT3 phosphorylation (Figure 1A) without inducing drop in body temperature or locomotor activity (Figures S1D and S1E). Finally, we pre-treated overnight fasted animals with the fatty acid amide hydrolase inhibitor URB-597 for 30 min and then treated them with leptin for 60 min. URB-597 selectively increased the concentration of the endocannabinoid anandamide in the basal

hypothalamus with no significant effect on 2-AG (Figure S1F) and, at the same time, shifted the correlation between plasma leptin and STAT3 phosphorylation to the right (Figure S1F). This finding suggests that the endogenous cannabinoid production machinery may be sufficient to suppress leptin signaling.

Altogether, activation of CB_1R impedes leptin-induced STAT3 signaling in the mediobasal hypothalamus without changing the accessibility of leptin to hypothalamic neurons or repressing leptin receptor expression.

Cannabinoids reduce leptin-initiated STAT3 signaling in cultured neuronal cells

The aforementioned *in vivo* experiments cannot precisely locate the CB_1R in the synaptic circuitry that conveys the cannabinoid inhibition of leptin signaling. Therefore, we tested whether the effect can be reproduced in homogeneous cell populations where CB_1Rs and leptin receptors are present in the same cell and synaptic connectivity is virtually absent. Highly differentiated hypothalamic GT1-7 neurons[26] and Neuro-2a neuroblastoma cells[27] expressing heterologous CB_1R and leptin receptors were stimulated with leptin in combination with DMSO or the CB_1R agonist ACEA. ACEA inhibited leptin-induced STAT3 tyrosine phosphorylation in both neuronal cells throughout a wide range of leptin concentrations (Figures 2A and 2B), implying that CB_1Rs can directly interfere with intracellular leptin signaling. (It has to be noted that no phosphorylation on S727 was observed in leptin stimulated cultured neurons [Figure S2F]).

At this point, we sought to replace labor-intensive western blotting with a high-yield method for monitoring leptin signaling. To this end, we established a semi-automated microscopic assay to monitor the translocation of fluorescently labeled STAT3 (STAT3-eGFP or STAT3-CFP-YFP) from the cytosol to the nucleus in cultured neurons. Stimulation with leptin brought about a time- and dose-dependent translocation of fluorescent STAT3 to the nucleus in Neuro 2a cells (Figure 2C and 2D). STAT3 nuclear translocation was expressed as the ratio of nuclear to perinuclear STAT3 fluorescence (Figure S2A); this parameter had comparable sensitivity and dynamic range to measuring the ratio of phosphorylated to total STAT3 by immunoblotting (Figure S2B).

Next, we determined that CB_1R activation not only impedes STAT3 phosphorylation but has a dampening effect on STAT3 nuclear translocation as well. The CB_1R agonists ACEA and HU 210 both blunted leptin-induced STAT3 nuclear translocation in Neuro 2a cells expressing heterologous CB_1Rs (Figures 2E and S2C). This inhibitory effect of the CB_1R agonists was blocked by the CB_1R inverse agonists AM 251 or rimonabant (Figure S2C). Furthermore, activation of endogenous CB_1Rs, expressed at low levels in untransfected Neuro 2a cells, was sufficient to impede leptin signaling, and silencing these endogenous CB_1Rs by siRNA treatment extinguished the cannabinoid-mediated inhibition on STAT3 (Figures S2D and S2E). Altogether, these data validate our translocation assay for the assessment of leptin-evoked STAT3 activation and demonstrate that cannabinoids antagonize leptin-initiated STAT signaling via the CB_1Rs of the leptin sensitive cell.

T cell protein tyrosine phosphatase conveys the cannabinoid-mediated inhibition of leptin signaling

Leptin and insulin signaling in the hypothalamus may be curtailed by the protein tyrosine phosphatases PTP1B (*PTP1N*) and TC-PTP (*PTP2N*; also referred to as TC45).[28] In Neuro 2a cells, the pan-phosphotyrosine phosphatase inhibitor sodium orthovanadate (Na_3VO_4) eliminated cannabinoid inhibition of leptin-induced STAT3 activation, and so did TCS 401, a dual PTP1B/TC-PTP inhibitor[29] (Figure 3A). However, the ACEA-evoked inhibition of STAT signaling was retained in the presence of the specific PTP1B inhibitor claramine[30] (Figure 3A) implying that CB_1R-evoked inhibition of STAT3 is mainly dependent on TC-PTP. The previous assumption was corroborated by the selective knockdown of PTP1B or TC-PTP with siRNA. Treatment with siRNA directed against PTP1B substantially increased the sensitivity of neuroblasts to leptin (Figure S3B), yet failed to affect the ability of ACEA to curtail leptin-induced STAT3 activation (Figure 3C). In contrast, silencing of TC-PTP, while marginally decreasing basal leptin sensitivity (Figure S3B), completely abolished the inhibitory cannabinoid effect on STAT3 signaling (Figure 3D). (Two separate siRNA sequences directed against TC-PTP gave harmonious results, only those obtained with sequence 2 are shown). These observations show that activation of CB_1Rs inhibits leptin-evoked STAT3 signaling in a TC-PTP dependent manner.

Attenuation of the leptin-initiated STAT3 response by cannabinoids involves β-arrestin1

In subsequent experiments, we aimed to determine which CB_1R signaling cascade recruits TC-PTP to diminish the leptin-evoked STAT3 response. Inhibition of membrane bound adenylyl cyclases via $G\alpha_i$ is a classic signal transduction pathway of the CB_1R.[31] As expected, the CB_1R agonist ACEA decreased

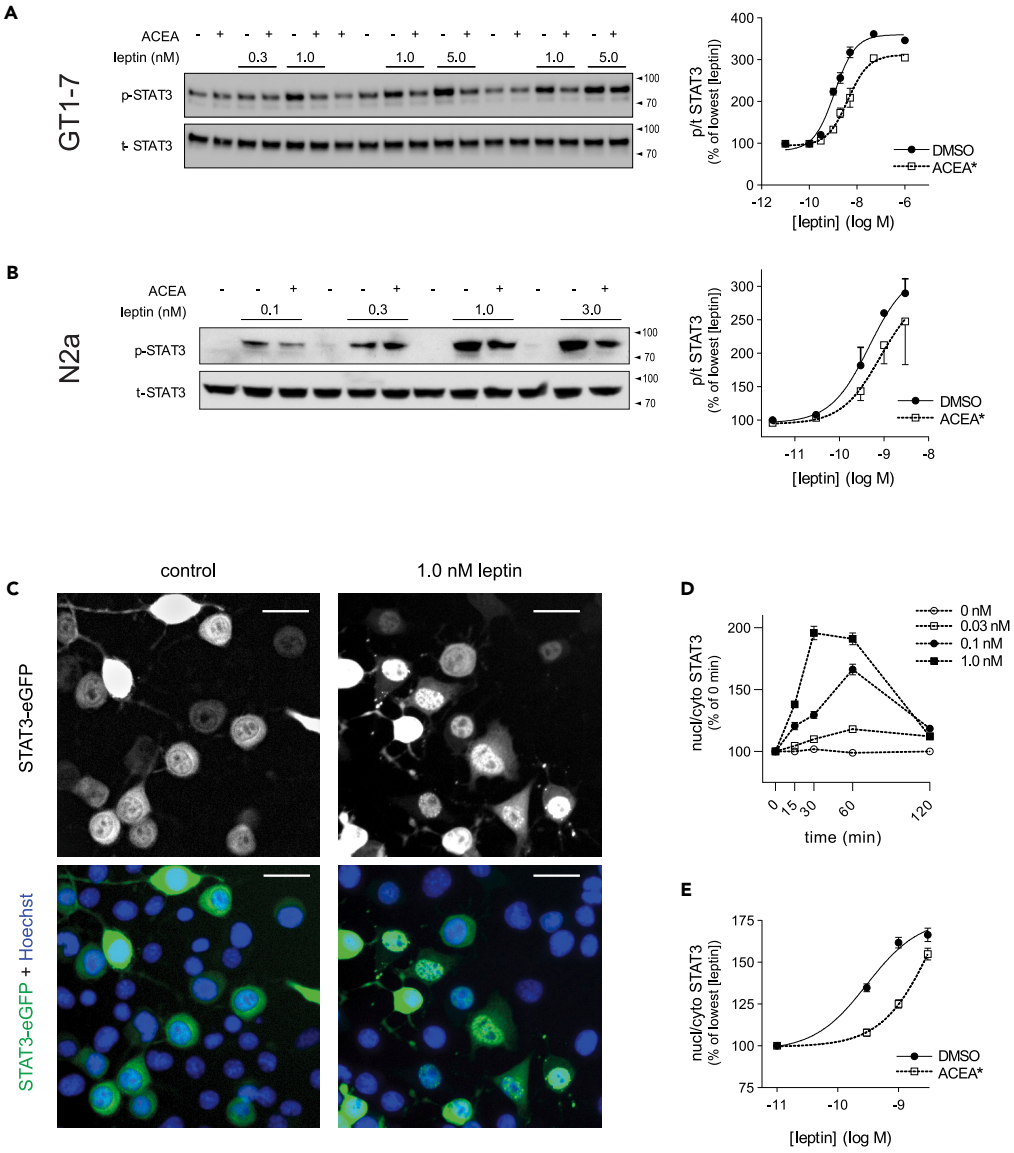

Figure 2. Cannabinoids reduce leptin-initiated STAT3 signaling in cultured neuronal cells

(A and B) Overnight serum starved GT1-7 (A) and Neuro 2a (B) cells expressing leptin and CB_1 receptors were concurrently stimulated with various concentrations of leptin and vehicle or ACEA (10 μM) for 15 min. STAT3 activation (phopho:total) was normalized to the average of lowest (leptin) + DMSO. Number of observation for *panel A* was 3 for all concentrations in both groups and for *panel B* (from lowest to highest [leptin]) n = 3-3-5-3-3 for DMSO and 3-3-6-3-3 for ACEA treated. *p < 0.0001 and p = 0.1 for the effect of ACEA in GT1-7 and in Neuro 2a cells, respectively (two-way ANOVA).

(C) Representative fluorescent confocal microscopic images of Neuro 2a cells expressing STAT3-eGFP (green) and nucleus stained with Hoechst 33342 (blue) and exposed to leptin for 45 min. Scale bars represent 25 μm. Note that in control cells many blue-stained nuclei are surrounded by green-stained (STAT3) cytosol, whereas in leptin-exposed cells many nuclei turn green with weaker green stain remaining in the cytosol.

(D) Dose and time dependency of STAT3 cytosol-to-nucleus translocation, as measured by automated confocal microscopy, in fluorescent STAT3 expressing Neuro 2a cells exposed to various concentrations of leptin for different lengths of time. Number of observations was between 160 and 680 per data point; p < 0.0001 for both the effect of time and leptin dose (two-way ANOVA).

(E) Leptin concentration—STAT3 translocation function as measured by confocal microscopy in Neuro 2a cells expressing transgenic leptin and CB_1 receptors and concurrently stimulated with leptin ± ACEA (2 μM) for 45 min n = 311–700 per point; *p < 0.0001 for the effect of ACEA (two-way ANOVA). (See also Figure S2).

Mean +, - or +/- S.E.M. are shown.

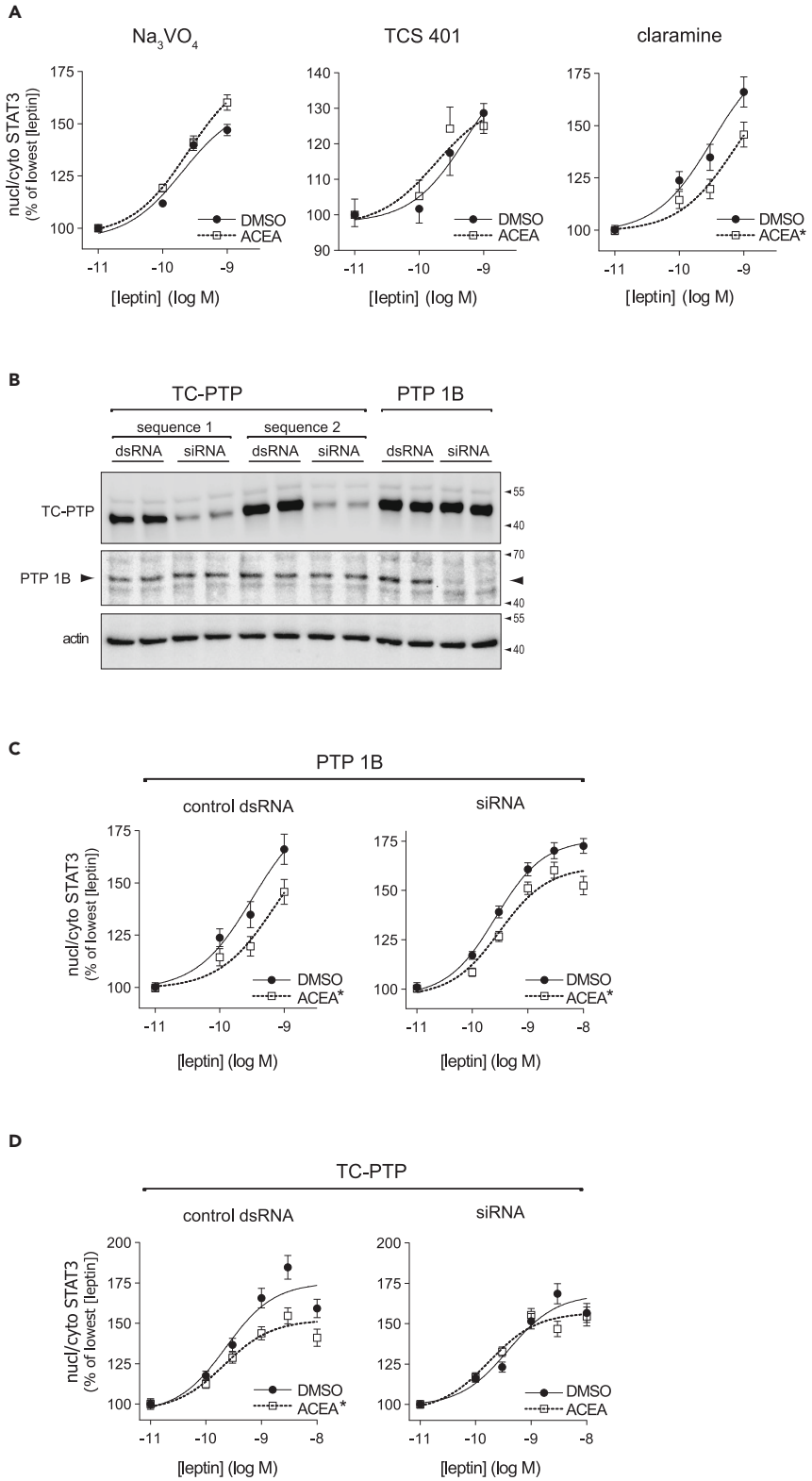

Figure 3. T cell protein tyrosine phosphatase conveys the cannabinoid-mediated inhibition of leptin signaling

(A) Neuro 2a cells were pre-incubated with different tyrosine phosphatase inhibitors (Na_3VO_4 100 μM, TCS 401 2 μM, claramine 10 μM) for 1 h and then were stimulated with various concentrations of leptin ± ACEA for 45 min. Nuclear

Figure 3. *Continued*
translocation of STAT3 was used as a measure of leptin signaling. n = between 80 and 731; *p < 0.002 for the effect of ACEA (two-way ANOVA).
(B) Neuro 2a cells were transfected with siRNA directed against TC-PTP (2 separate siRNA sequences) or PTP1B or with respective control non-silencing dsRNAs, and TC-PTP and PTP1B protein levels were assessed by Western blotting.
(C and D) Neuro 2a cells expressing fluorescently labeled STAT3 were treated with siRNA directed against TC-PTP (sequence 2) or PTP1B and were stimulated with leptin ± ACEA or DMSO for 45 min. STAT3 nuclear translocation as a function of leptin concentration is shown. n = 183–1127 cells per point, *p < 0.0001 for the effect of ACEA (two-way ANOVA). (See also Figure S3).
Mean +/- S.E.M. are shown.

cytosolic cAMP concentration in a pertussis toxin dependent manner (Figure S4A). Nonetheless, the inhibition of leptin-initiated STAT3 signaling by cannabinoids was retained in pertussis toxin pre-treated neurons (Figure S4B), strongly arguing against the involvement of the $G\alpha_i$—cAMP pathway in the inhibition of STAT3.

β-arrestins coordinate some of the $G\alpha_i$ independent pathways of CB_1R signaling.[32] In line with previous observations,[33] we detected CB_1R—β-arrestin2 interaction upon CB_1R stimulation by means of bioluminescence resonance energy transfer (BRET) (Figure S4C). Yet, the selective knockdown of β-arrestin2 did not affect the ability of CB_1Rs to suppress leptin-stimulated STAT3 signaling (Figures 4A and 4B). Knocking down β-arrestin1 expression with siRNA, on the other hand, practically eliminated cannabinoid suppression of leptin signaling, as demonstrated by both western blotting and the STAT3 translocation assay (Figures 4A, 4B, and 4C). In addition, selective rescue of β-arrestin1 expression in β-arrestin1+2 double knockout HEK 293 cells restored cannabinoid-mediated inhibition of leptin signaling (Figure 4D).

It was reported that β-arrestin1 binds nuclear STAT1 and, in so doing, enables STAT1 dephosphorylation in interferon-stimulated non-neuronal cells.[34] In agreement with such a mechanism, we observed partial translocation of β-arrestin1, but not that of β-arrestin2, to the nucleus upon CB_1R stimulation (Figure S4D). Moreover, β-arrestin1 could bind both STAT3 and TC-PTP, but not PTP1B, as indicated by co-immunoprecipitation (Figure S4E). Altogether, these data show that β-arrestin1 is required for the cannabinoid-dependent inhibition of STAT3 signaling and that β-arrestin1 may directly interact with both STAT3 and TC-PTP.

Feeding-induced hypothalamic signaling by endogenous leptin is impeded by CB_1R activation in a β-arrestin1-dependent manner

Our results so far indicate that STAT3 phosphorylation by exogenous leptin is inhibited by CB_1R activation both in mice *in vivo* and in neural cell lines *in vitro*, and findings in the latter paradigm indicate that this CB_1R-mediated effect is dependent on TC-PTP and β-arrestin1. Next, we aimed to test whether CB_1R activation attenuates leptin signaling also during *physiological* elevations of the hormone elicited by refeeding fasted animals (Figure 5A). Re-introducing food to overnight fasted mice elicited robust STAT3 activation in the arcuate nucleus as demonstrated by both immunohistochemistry and western blotting (Figures 5B and 5C, respectively). Circulating leptin also readily responded to food intake (Figure 5C). While the CB_1R agonist ACEA had no effect on the rise in plasma leptin, it significantly reduced STAT3 phosphorylation in the hypothalamus (Figure 5C). Importantly, the feeding-induced hypothalamic leptin response was insensitive to CB_1R activation in $CB_1R^{-/-}$ or β-arrestin1$^{-/-}$ animals (Figures 5C and 5D). Taken together, acute CB_1R activation reduces the responsiveness of the basal hypothalamus to physiological elevations of leptin and this effect is dependent on β-arrestin1.

DISCUSSION

Activation of CB_1Rs increases food intake, reduces energy expenditure, and promotes adipose tissue expansion via pleiotropic actions throughout the CNS and peripheral organs.[12,35] In the CNS, the majority of CB_1Rs reside on presynaptic terminals[36] and the metabolic effects of cannabinoids are believed to be conveyed primarily by these presynaptic CB_1Rs, via the modulation of classical neurotransmission (reviewed in[11]). Beside such modulatory actions, we report here that CB_1R activation can also *directly* target the signal transduction of the main anorexigenic hormone, leptin. More specifically, activation of CB_1Rs of the leptin sensitive cell inhibits leptin receptor signaling by prompting the dephosphorylation of STAT3 on its crucial tyrosine residue (Y705).

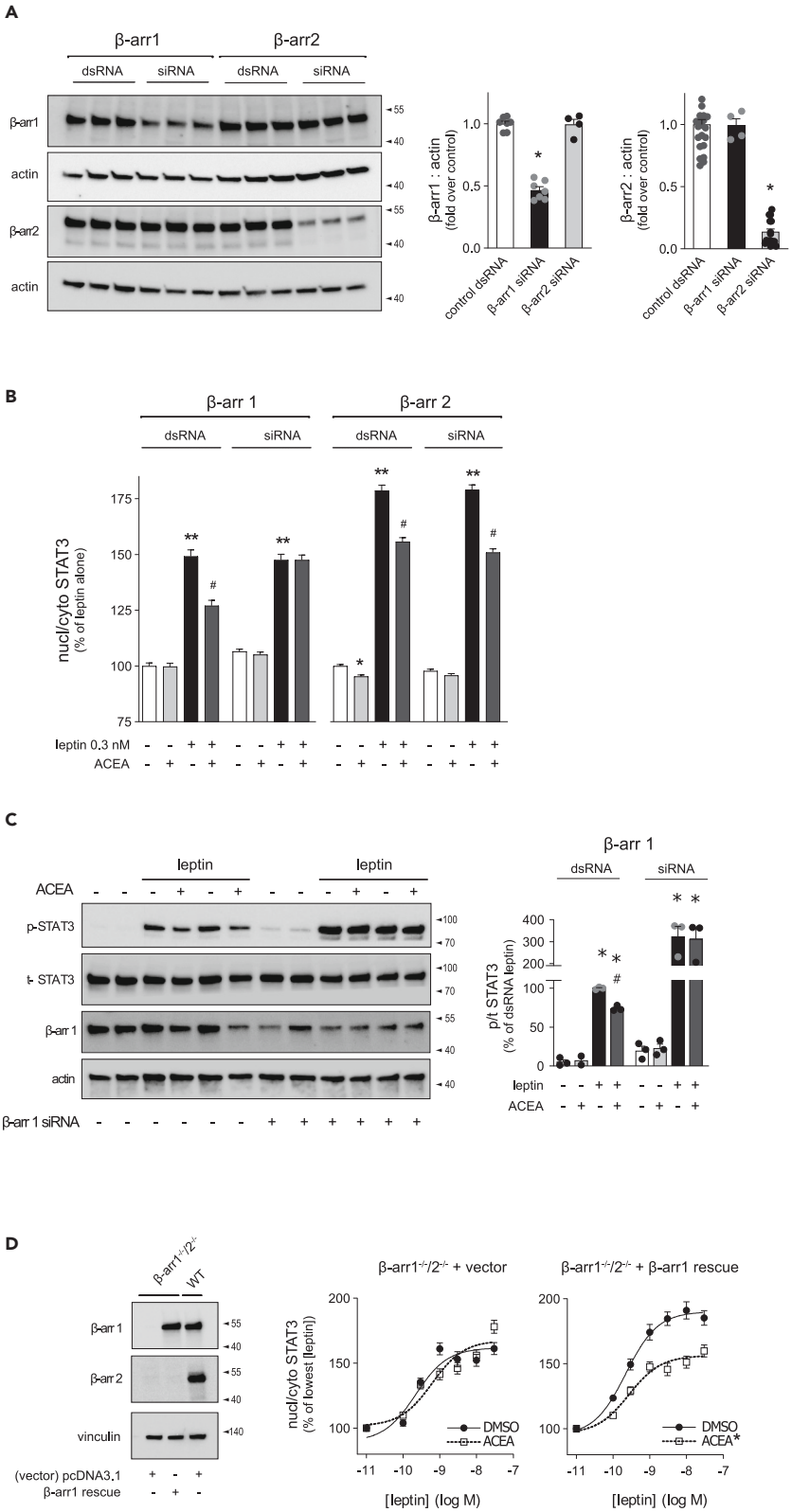
A
β-arr1
β-arr2
dsRNA
siRNA
β-arr1
actin
β-arr2
actin
β-arr1 : actin (fold over control)
β-arr2 : actin (fold over control)
control dsRNA
β-arr1 siRNA
β-arr2 siRNA
B
β-arr 1
β-arr 2
nucl/cyto STAT3 (% of leptin alone)
leptin 0.3 nM
ACEA
C
leptin
ACEA
p-STAT3
t- STAT3
β-arr 1
actin
β-arr 1 siRNA
p/t STAT3 (% of dsRNA leptin)
D
β-arr1-/-/2-/-
WT
β-arr 1
β-arr 2
vinculin
(vector) pcDNA3.1
β-arr1 rescue
β-arr1-/-/2-/- + vector
β-arr1-/-/2-/- + β-arr1 rescue
nucl/cyto STAT3 (% of lowest [leptin])
DMSO
ACEA
[leptin] (log M)

Figure 4. Attenuation of the leptin-initiated STAT3 response by cannabinoids involves β-arrestin1

(A) Immunoblot analysis of β-arrestin1 and β-arrestin2 siRNA treatment on protein abundance. Neuro 2a cells were transfected with siRNA directed against murine β-arrestin1 (*arrb1*, βarr1) or β-arrestin2 (*arrb2*, βarr2) or with control (non-silencing) dsRNA as appropriate. Cells were subjected to western blot and β-arrestin to actin protein abundance was normalized to that in the control dsRNA treated group. n = 7-7-4 (left bar graph, L to R) and 24-18-4 (right bar graph, L to R); *p < 0.001 vs. control dsRNA (ANOVA with Holm-Sidak's multiple comparisons test).

(B) Analysis of leptin-induced STAT3 nuclear translocation in Neuro 2a cells expressing both ObR_b and CB_1 receptors and transfected with β-arrestin1 or β-arrestin2 siRNA or respective non-silencing control dsRNAs. Cells were stimulated with leptin ± ACEA for 45 min as indicated. Numbers of observations were between 450 and 2000 STAT3-GFP^+ cells/group. *p = 0.011 and **p < 0.0001 when compared to $leptin^-/ACEA^-$ within the quadruplicate treated with the same RNA; $^{\#}$p < 0.0001 when compared to $leptin^+/ACEA^-$ of the same RNA treated quadruplicate (Kruskal-Wallis ANOVA followed by Dunn's test). For a more detailed representation of the same data, please refer to the violin plot graph in Fig.S4F.

(C) Effect of β-arrestin1 knockdown on the cannabinoid sensitivity of leptin-stimulated STAT3 phosphorylation. Neuro 2a cells expressing both ObR_b and CB_1 receptors were transfected with control dsRNA or siRNA directed against murine β-arrestin1 and stimulated with 100 p.m. leptin ±2 μM ACEA for 60 min n = 3–7/group, *p < 0.01 vs. control RNA and $^{\#}$p < 0.01 when compared to $leptin^+/ACEA^-$ (ANOVA with Holm-Sidak's multiple comparisons test, data obtained from 2 independent experiments).

(D) β-arrestin1/2 double knockout or WT HEK 293 cells were transfected with empty plasmid (pcDNA3.1[+]) or with a plasmid coding for β-arrestin1 as indicated and subjected to immunoblotting (blot representative for 3 independent experiments) or to STAT3 translocation assay. Number of observations for the translocation experiments were 482–1784 cells per data point, *p < 0.0001 for the effect of ACEA (two-way ANOVA). (See also Figure S4).

Mean + or +/- S.E.M. are shown.

We found that in lean wild-type mice, following the administration of a low pharmacological dose of recombinant leptin, hypothalamic leptin signaling was attenuated by the concurrent activation of CB_1Rs. To avoid supraphysiological effects of pharmacological leptin doses, and to confine leptin responses to the physiological targets of the hormone, we took advantage of the fasting—refeeding paradigm and the small increases in plasma leptin it elicits. The refeeding-evoked STAT3 response in the mediobasal hypothalamus was reduced by CB_1R activation in wild-type mice, but not in $CB_1R^{-/-}$ animals, showing that signaling by endogenous leptin in the *physiological* concentration range is in fact susceptible to cannabinoid-mediated inhibition. This gives our observation a broader biological relevance.

In principle, numerous mechanisms could account for reduced central leptin sensitivity *in vivo*. Impaired leptin transport across the blood-brain barrier[37]; induction of the classical inhibitor of leptin signaling, SOCS3[38]; repression of the leptin receptor; and CB_1R-induced hypothermia as well as catalepsy may all potentially modify responsiveness to leptin. However, in our paradigms CB_1R activation did not influence plasma or cerebrospinal fluid leptin concentrations, *Lepr* or *Socs3* expression, and low doses of ACEA with no hypothermic and cataleptic effects were still able to supress leptin signaling. Thus, we concluded that cannabinoids most probably target the signal transduction of the leptin receptor directly, rather than interfering with pre-receptor processes. This notion was corroborated by the finding that the CB_1R agonists ACEA and HU 210 suppress the leptin-evoked STAT3 response in cultured neurons, *i.e.* in the absence of complex synaptic connections. This observation strongly argues that the leptin responsive cell's own somatodentritic CB_1Rs[39] are sufficient for the inhibitory effect and validated the use of neuronal cultures in subsequent experiments.

Cultured neurons offered several methodological advantages in our study (i) phospho-STAT3 immunoreactivity from leptin sensitive astrocytes[40]; was naturally eliminated in neuronal cultures; (ii) the number of animals necessary for the study could be reduced: (iii) cultured cells allowed for the semi-automated confocal microscopic measurement of leptin signaling. This assay takes advantage of the accumulation of STAT3 dimers in the nucleus after leptin receptor activation. The nuclear to cytoplasmic ratio of STAT3 corresponds to its overall biological activity[41] and closely parallels its phosphorylation state (Figure S2B). Like its phosphorylation, leptin-evoked nuclear accumulation of STAT3 also proved to be sensitive to inhibition by CB_1R agonists, validating the *in vitro* translocation assay for further experimentation.

It has been shown that TC-PTP (T cell protein tyrosine phosphatase, PTPN2, or TC45) and the closely related phosphatase PTP1B may contribute to leptin resistance.[42] Indeed, genetic ablation or pharmacological blockade of these phosphatases in the hypothalamus prevents or reduces diet-induced obesity by supressing food intake, supporting adipose tissue browning and boosting energy expenditure in mouse models of diet-induced obesity.[28] Consistent with such a role of these phosphatases, in our *in vitro* paradigms PTP1B increased basal leptin sensitivity, and TC-PTP was essential for the CB_1R-mediated inhibition leptin signaling.

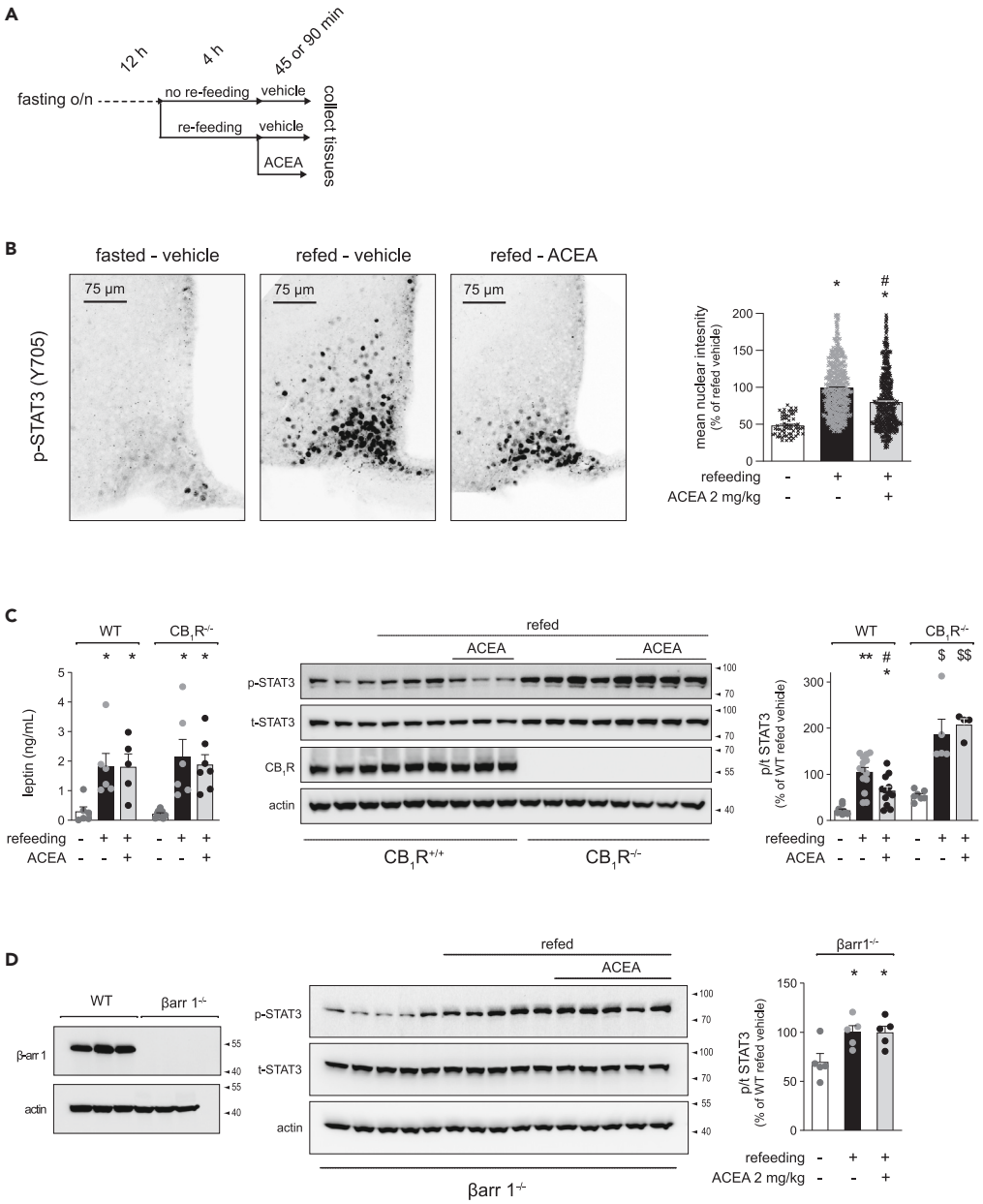

Figure 5. Feeding-induced hypothalamic signaling by endogenous leptin is impeded by CB_1R activation in a β-arrestin1-dependent manner

(A) Scheme of the fasting-refeeding paradigm. After an overnight fast, food was made available *ad libitum* for 2 or 4 h. Then, food was again removed and mice were treated with the CB_1R agonist ACEA (2 or 10 µM, *i.p.*) or with vehicle for 45 or 90 min and then euthanized under anesthesia.

(B) Immunohistochemical analysis of phospho-STAT3 in the arcuate nucleus (approx. bregma −2 mm). n = 64–594-586 phospho-STAT3$^+$ nuclei (L to R) from 4-6-6 animals (respectively); *p < 0.0001 vs. non-refed group and p#<0.0001 vs. refeeding$^+$/ACEA$^-$ (ANOVA followed by Kruskal-Wallis *post-hoc* test).

(C) *Left bar graph*: serum leptin concentration in WT and CB_1R knockout animals subjected to the fasting-refeeding paradigm; n = 6-6-5-9-6-7 (L to R); *p < 0.05 and **p < 0.01 compared to refeeding$^-$/ACEA$^-$ group of the same genetic background (ANOVA with Kruskal-Wallis *post-hoc* test). *Middle panel*: representative western blot showing hypothalamic STAT3 activation in WT and $CB_1R^{-/-}$ animals. *Right panel*: statistical analysis of pooled western blot data; n = 11–14-12-7-5-4 (L to R); **p < 0.001 and *p < 0.01 vs. WT non-refed group, $^{\#}$p < 0.01 vs. refeeding$^+$/ACEA$^-$, $^{\$\$}$p < 0.01 and $^{\$}$p < 0.05 compared to $CB_1R^{-/-}$ non-refed group (ANOVA and Holm-Sidak's or Dunn's *post-hoc* tests).

Figure 5. *Continued*

(D) Hypothalamic β-arrestin1 expression (left panel) and STAT3 activation (middle and right panels) in fasting-refeeding experiments in β-arrestin1 knockout mice. Number of observations was 5 in all groups; *p < 0.039 vs. non-refed group (ANOVA and Sidak's *post-hoc* test).

Mean + S.E.M. are shown.

While TC-PTP had only a slight modulatory effect on leptin sensitivity without CB_1R activation, it substantially reduced the leptin-evoked STAT3 response upon CB_1R agonist treatment (*cf.* Figures 3D and S3B). The possibility that silencing TCPTP may inhibit the leptin response and thus pre-empt the similar action of ACEA is unlikely in view of published findings that leptin sensitivity is inhibited by an excess rather than a deficiency in TCPTP activity.[42,43] By contrast, PTP1B decreased the responsiveness of cultured neurons to leptin but did so in a CB_1R independent manner (*cf.* Figures 3C and S3B). These findings suggest that PTP1B, in accordance with previous reports,[44] exerts tonic suppression on leptin signaling while TC-PTP antagonizes STAT3 only when recruited by CB1R activation. It should be noted here that the non-specific phosphatase inhibitors orthovanadate and TCS 401 did not increase leptin sensitivity in the absence of CB_1R agonists, although both inhibitors are expected to block both TC-PTP *and* PTP1B. We suspect that this phenomenon may be due to their possibly numerous effects on other phosphatases. This observation also underlines the importance of corroborating pharmacological findings with more specific genetic approaches such as, in this study, siRNA mediated knockdown.

CB_1Rs couple predominantly to $G_{i/o}$ heterotrimeric G-proteins[31]; however, decoupling CB_1Rs from the $G_{i/o}$ protein with pertussis toxin did not affect cannabinoid suppression of STAT3 implying that $G_{i/o}$ dependent cascades are not essential for this inhibitory effect. It is noteworthy, however, that the synthetic cannabinoid HU 210 was shown to trigger STAT3 and Src kinase phosphorylation in Neuro 2a cells in a $G_{i/o}$ dependent manner.[45] While this signaling pathway may have long-term effects on neurite outgrowth in neuroblasts,[45] it did not contribute to CB_1R-mediated inhibition of leptin signaling, as this latter proved to be $G_{i/o}$ independent. CB_1Rs also signal via β-arrestins, with β-arrestin1 typically mediating long-term effects on the MAPK cascade,[46] and β-arrestin2 primarily governing receptor internalization.[33] In our hands, CB_1Rs clearly engaged β-arrestin2 upon activation, yet, only β-arrestin1 proved to be essential for the cannabinoid-mediated inhibition of leptin signaling. Such non-redundancy between β-arrestin1 and β-arrestin2 is in keeping with the notion that different β-arrestins have divergent functions under most conditions.[47,48] For instance, β-arrestin2, but not β-arrestin1, was found to be involved in the CB_1R-induced inhibition of insulin-stimulated glucose uptake into skeletal muscle,[49] whereas β-arrestin1 was found to convey the pro-fibrogenic effect of CB_1Rs in the liver.[50]

Notably, knockdown of β-arrestin1 in Neuro 2a cells markedly increased leptin-induced pSTAT3 levels (Figure 4C), and a similar tendency was evident *in vivo* in $CB_1R^{-/-}$ compared to wild-type mice (Figures 1A and 5C), suggesting that leptin signaling may be tonically inhibited by endocannabinoids via a CB_1R/β-arrestin1 pathway even under basal conditions. This model is in harmony with the well documented phenotype of mice lacking CB_1R which are highly leptin sensitive, slightly hypophagic, and resistant to diet-induced obesity.[13] On the other hand, mice lacking β-arrestin1 in specifically AgRP neurons are not protected against diet-induced obesity and exhibit reduced hypothalamic insulin sensitivity. The most probable explanation is that β-arrestin1 binds and stabilizes insulin receptor substrate-1 (IRS-1).[51] and is therefore required for normal central insulin sensitivity. Since the leptin receptor is thought to couple to IRS-2/4,[6] we suppose that β-arrestin1 may influence central insulin and leptin signaling differently.

Antimicrobial signaling, mediated by STAT1, was found to be attenuated by a concerted action of β-arrestin1 and TC-PTP in mammalian epithelial cells[34] and in non-vertebrate immune cells[52] (but see[53]). Our findings reveal an analogous mechanism and extend it to leptin-evoked STAT3 signaling in neurons since (i) a portion of β-arrestin1 translocated to the nucleus upon CB_1R stimulation; (ii) β-arrestin1 bound a measurable fraction of the STAT3 pool; (iii) a detectable amount of TC-PTP could be also co-immunoprecipitated with β-arrestin1; (iv) TC-PTP was essential for the cannabinoid-mediated inhibition of STAT3; and finally, (v) CB_1R activation was unable to suppress hypothalamic pSTAT3 in β-arrestin1 knockout mice, confirming the β-arrestin1 dependence of this inhibitory pathway *in vivo*. However, the present work reveals that, as opposed to STAT1, inhibition of the leptin-induced STAT3 response by β-arrestin1/TC-PTP is not a constant but an "on-demand" process that can be deployed by cannabinoids.

Triggering β-arrestin1 redistribution may not be unique to CB_1Rs as opioid receptors may also trigger the translocation of β-arrestin1 to the nucleus.[54] However, CB_1R activation alone induced only a moderate

translocation of β-arrestin1 to the nucleus. Instead, it was the concurrent activation of both CB1Rs and leptin receptors that was highly effective in this respect. This pattern is similar to that observed with co-immunoprecipitation, where co-stimulation the leptin receptors and CB_1Rs was required to increase the amount of the β-arrestin1/STAT3/TC-PTP complex. This implies that active leptin receptor signaling is also required for efficient CB_1R mediated β-arrestin1 translocation and, subsequently, for the signaling complex to form in a biologically meaningful extent.

Whereas the importance of tyrosine phosphorylation of STAT3 is well recognized, the relevance of phosphorylation on serine residues is less clear.[6] Importantly, phosphorylation of STAT3 at S727 was found to accelerate its inactivation,[55] and Morello and colleagues demonstrated that endocannabinoids bring about S727 phosphorylation of STAT3 in POMC neurons.[56] This process may be complementary to, but is most likely distinct from the hereby reported phenomenon since we did not observe serine phosphorylation of STAT3 upon leptin receptor and/or CB_1R activation in any of the relevant paradigms (Figures S1G, S1H, and S2F). On the other hand, genetic ablation of CB_1Rs in hepatocytes increases their leptin sensitivity[57]; a mechanism similar to the one reported here may be responsible for this effect.

Visceral obesity is associated with leptin resistance[7] and increased activity of the endocannabinoid/CB_1R system.[12] Consistently, the CB_1R inverse agonist rimonabant mitigates visceral obesity and its metabolic complications[58] but its clinical use has been thwarted by neuropsychiatric side effects[4] mediated via CB_1R blockade in the brain. This limitation could be overcome with peripherally restricted CB_1R antagonists devoid of CNS effects[15] or with the application of CB_1R biased antagonists. We have recently shown in obese mice that MRI-1891, a CB_1R antagonist that preferentially inhibits CB_1R-mediated β-arrestin2 recruitment, restores hyperleptinemia, muscle insulin sensitivity and reduces food intake without exerting anxiogenic side effects even at partial brain CB_1R occupancy.[49] This finding together with our present data support the idea that β-arrestin biased CB_1R antagonists may be used to mitigate obesity and its metabolic corollaries without eliciting adverse neurobehavioral effects.

All in all, in this study we demonstrate that the hypothalamic response to physiological elevations of leptin is mitigated by CB_1R agonists. Upon CB_1R activation, β-arrestin1 recruits TC-PTP to dephosphorylate STAT3. This mechanism is expected to become more pronounced when hypothalamic endocannabinoid levels and/or TC-PTP expression increase, such as during fasting[59,60] or in diet-induced obesity.[8] Limiting leptin's central effects may have long term impact on food intake, energy expenditure and body weight, and it may be speculated that the CB_1R-medited STAT3 inhibition contributes to the development of leptin resistance and ensuing obesity. However, further studies are necessary to put the hereby described phenomenon into broader physiological and pathophysiological context.

Limitations of the study

The present study demonstrates that the acute activation of CB_1Rs inhibits leptin-evoked STAT3 signaling via a concerted action of β-arrestin1 and TC-PTP . In the present study we focused our investigation on STAT3 signaling, as it conveys the classic anorectic actions of leptin. However, leptin receptors also initiate MAPK, PI3K-Akt-mTOR signaling, and modulate AMPK activity, all of which have physiological/pathophysiological significance. Therefore, whether cannabinoids also modulate those pathways will need to be explored in the future. Also, in the present work we investigated male animals only. As ovarian steroids modulate hypothalamic leptin signaling pathways in a complex manner,[61,62] our proposed model may work differently in females. Future studies will need to address these questions to be able to extrapolate the present findings to the level of systemic metabolism and to the female sex.

STAR★METHODS

Detailed methods are provided in the online version of this paper and include the following:

- KEY RESOURCES TABLE
- RESOURCE AVAILABILITY
  - Lead contact
  - Materials availability
  - Data and code availability
- EXPERIMENTAL MODEL AND STUDY PARTICIPANT DETAILS
  - Ethics statement and animal experiments

SUPPLEMENTAL INFORMATION

Supplemental information can be found online at https://doi.org/10.1016/j.isci.2023.107207.

ACKNOWLEDGMENTS

We are indebted to Dr. Katalin Erdélyi (National Institute of Oncology, Budapest, Hungary), Dr. Pál Pacher (NIAAA, NIH, Rockville, MD, USA), Dr. Balázs Enyedi (Semmelweis University, Budapest, Hungary) and Dr. Zoltán Hegyi (Bio-Science, Budapest, Hungary) for technical help and valuable discussion. GT1-7 cells were kindly provided by Dr. Pamela L. Mellon (University of California, San Diego, CA, USA). The authors thank Dr. Gerhard Müller-Newen (University Hospital Aachen, Aachen, Germany) for generously providing the STAT3-CFP-YFP construct and Dr. Tamás Balla (NICHD, NIH, Bethesda, MD, USA) for his help in construct design and production. The CFP-tagged mouse leptin receptor clone was a generous gift from Dr. Arieh Gertler (The Hebrew University of Jerusalem, Rehovot, Israel). We are indebted to Dr. Erzsébet Ligeti and Dr. Roland Csépányi-Kömi (Semmelweis University, Budapest, Hungary) for providing resources for molecular biological work.

This work was supported by the following grants: National Research, Development and Innovation Office grants NKFI-6/FK_124038 to G. Szanda, intramural NIH funds to G. Kunos and FK_18/128376 to É.W. (PI: Roland Csépányi-Kömi). The work was also funded by the Scientific and Innovation Fund of the Semmelweis University, Budapest, Hungary (26303/AOELT/2019; to G.S.) and the Eötvös Loránd Research Network (to ELKH-SE Laboratory of Molecular Physiology Research Group). G. Szanda was supported by the János Bólyai Research Scholarship of the Hungarian Academy of Sciences. The high-content imaging system was procured using Hungarian National Competitiveness and Excellence Programme funds (NVKP_16-1-2016-0039).

The Servier Medical Art Collection (https://smart.servier.com/) was used for the preparation of the graphical abstract.

AUTHOR CONTRIBUTIONS

Conceptualization G.S. and G.K.; Methodology G.S., T.J., J.T., R.C., and G.K.; Formal Analysis G.S., A.S., E.S-K., A.D.T., and G.K., Investigation G.S., T.J., R.C., G.G., A.R., J.L., L.C., B.S., E.S-K., A.D.T., V.B.H., and J.T.; Resources G.S., E.W., L.H., A.I., and G.K.; Writing – Original Draft G.S. and G.K.; Writing – Review & Editing G.S., T.J., A.S., A.D.T., J.T., and G.K., Visualization G.S.; Supervision G.S. and G.K.; Funding Acquisition G.S., L.H., and G.K. All authors had access to the manuscript and agreed with the final version.

DECLARATION OF INTERESTS

The authors declare no competing interest.

INCLUSION AND DIVERSITY

We support inclusive, diverse and equitable conduct of research.

Received: January 26, 2023
Revised: May 20, 2023
Accepted: June 21, 2023
Published: June 25, 2023

REFERENCES

1. Hill, J.O., Wyatt, H.R., and Peters, J.C. (2012). Energy balance and obesity. Circulation *126*, 126–132. https://doi.org/10.1161/CIRCULATIONAHA.111.087213.

2. World Health Organization. (2020). Fact sheet: obesity and overweight. https://www.who.int/en/news-room/fact-sheets/detail/obesity-and-overweight.

3. Srivastava, G., and Apovian, C.M. (2018). Current pharmacotherapy for obesity. Nat. Rev. Endocrinol. *14*, 12–24. https://doi.org/10.1038/nrendo.2017.122.

4. Christensen, R., Kristensen, P.K., Bartels, E.M., Bliddal, H., and Astrup, A. (2007). Efficacy and safety of the weight-loss drug rimonabant: a meta-analysis of randomised trials. Lancet (London, England) *370*, 1706–1713. https://doi.org/10.1016/s0140-6736(07)61721-8.

5. Zhang, Y., Proenca, R., Maffei, M., Barone, M., Leopold, L., and Friedman, J.M. (1994). Positional cloning of the mouse obese gene and its human homologue. Nature *372*, 425–432. https://doi.org/10.1038/372425a0.

6. Wauman, J., and Tavernier, J. (2011). Leptin receptor signaling: pathways to leptin resistance. Front. Biosci. *16*, 2771–2793.

7. Engin, A. (2017). Diet-Induced Obesity and the Mechanism of Leptin Resistance. Adv. Exp. Med. Biol. *960*, 381–397. https://doi.org/10.1007/978-3-319-48382-5_16.

8. Tam, J., Szanda, G., Drori, A., Liu, Z., Cinar, R., Kashiwaya, Y., Reitman, M.L., and Kunos, G. (2017). Peripheral cannabinoid-1 receptor blockade restores hypothalamic leptin signaling. Mol. Metabol. *6*, 1113–1125. https://doi.org/10.1016/j.molmet.2017.06.010.

9. Pacher, P., Bátkai, S., and Kunos, G. (2006). The endocannabinoid system as an emerging target of pharmacotherapy. Pharmacol. Rev. *58*, 389–462. https://doi.org/10.1124/pr.58.3.2.

10. Koch, M. (2017). Cannabinoid Receptor Signaling in Central Regulation of Feeding Behavior: A Mini-Review. Front. Neurosci. *11*, 293.

11. Lau, B.K., Cota, D., Cristino, L., and Borgland, S.L. (2017). Endocannabinoid modulation of homeostatic and non-homeostatic feeding circuits. Neuropharmacology *124*, 38–51. https://doi.org/10.1016/j.neuropharm.2017.05.033.

12. Jourdan, T., Degrace, P., González-Mariscal, I., Szanda, G., and Tam, J. (2020). Chapter 15 - Endocannabinoids: the lipid effectors of metabolic regulation in health and disease. In Lipid Signaling and Metabolism, J.M. Ntambi, ed. (Academic Press), pp. 297–320. https://doi.org/10.1016/B978-0-12-819404-1.00015-4.

13. Ravinet Trillou, C., Delgorge, C., Menet, C., Arnone, M., and Soubrié, P. (2004). CB1 cannabinoid receptor knockout in mice leads to leanness, resistance to diet-induced obesity and enhanced leptin sensitivity. Int. J. Obes. Relat. Metab. Disord. *28*, 640–648. https://doi.org/10.1038/sj.ijo.0802583.

14. Pi-Sunyer, F.X., Aronne, L.J., Heshmati, H.M., Devin, J., and Rosenstock, J.; RIO-North America Study Group (2006). Effect of rimonabant, a cannabinoid-1 receptor blocker, on weight and cardiometabolic risk factors in overweight or obese patients: RIO-North America: a randomized controlled trial. JAMA *295*, 761–775. https://doi.org/10.1001/jama.295.7.761.

15. Tam, J., Cinar, R., Liu, J., Godlewski, G., Wesley, D., Jourdan, T., Szanda, G., Mukhopadhyay, B., Chedester, L., Liow, J.S., et al. (2012). Peripheral cannabinoid-1 receptor inverse agonism reduces obesity by reversing leptin resistance. Cell Metabol. *16*, 167–179. https://doi.org/10.1016/j.cmet.2012.07.002.

16. Di Marzo, V., Goparaju, S.K., Wang, L., Liu, J., Bátkai, S., Járai, Z., Fezza, F., Miura, G.I., Palmiter, R.D., Sugiura, T., and Kunos, G. (2001). Leptin-regulated endocannabinoids are involved in maintaining food intake. Nature *410*, 822–825. https://doi.org/10.1038/35071088.

17. Malcher-Lopes, R., Di, S., Marcheselli, V.S., Weng, F.J., Stuart, C.T., Bazan, N.G., and Tasker, J.G. (2006). Opposing crosstalk between leptin and glucocorticoids rapidly modulates synaptic excitation via endocannabinoid release. J. Neurosci. *26*, 6643–6650. https://doi.org/10.1523/jneurosci.5126-05.2006.

18. Cardinal, P., Bellocchio, L., Clark, S., Cannich, A., Klugmann, M., Lutz, B., Marsicano, G., and Cota, D. (2012). Hypothalamic CB1 cannabinoid receptors regulate energy balance in mice. Endocrinology *153*, 4136–4143. https://doi.org/10.1210/en.2012-1405.

19. Jo, Y.H., Chen, Y.J.J., Chua, S.C., Jr., Talmage, D.A., and Role, L.W. (2005). Integration of endocannabinoid and leptin signaling in an appetite-related neural circuit. Neuron *48*, 1055–1066. https://doi.org/10.1016/j.neuron.2005.10.021.

20. Cristino, L., Busetto, G., Imperatore, R., Ferrandino, I., Palomba, L., Silvestri, C., Petrosino, S., Orlando, P., Bentivoglio, M., Mackie, K., and Di Marzo, V. (2013). Obesity-driven synaptic remodeling affects endocannabinoid control of orexinergic neurons. Proc. Natl. Acad. Sci. USA *110*, E2229–E2238. https://doi.org/10.1073/pnas.1219485110.

21. Cardinal, P., André, C., Quarta, C., Bellocchio, L., Clark, S., Elie, M., Leste-Lasserre, T., Maitre, M., Gonzales, D., Cannich, A., et al. (2014). CB1 cannabinoid receptor in SF1-expressing neurons of the ventromedial hypothalamus determines metabolic responses to diet and leptin. Mol. Metabol. *3*, 705–716. https://doi.org/10.1016/j.molmet.2014.07.004.

22. Palomba, L., Silvestri, C., Imperatore, R., Morello, G., Piscitelli, F., Martella, A., Cristino, L., and Di Marzo, V. (2015). Negative Regulation of Leptin-induced Reactive Oxygen Species (ROS) Formation by Cannabinoid CB1 Receptor Activation in Hypothalamic Neurons. J. Biol. Chem. *290*, 13669–13677. https://doi.org/10.1074/jbc.M115.646885.

23. Münzberg, H., Flier, J.S., and Bjørbaek, C. (2004). Region-specific leptin resistance within the hypothalamus of diet-induced obese mice. Endocrinology *145*, 4880–4889. https://doi.org/10.1210/en.2004-0726.

24. Hillard, C.J., Manna, S., Greenberg, M.J., DiCamelli, R., Ross, R.A., Stevenson, L.A., Murphy, V., Pertwee, R.G., and Campbell, W.B. (1999). Synthesis and characterization of potent and selective agonists of the neuronal cannabinoid receptor (CB1). J. Pharmacol. Exp. Therapeut. *289*, 1427–1433.

25. Bjørbaek, C., El-Haschimi, K., Frantz, J.D., and Flier, J.S. (1999). The role of SOCS-3 in leptin signaling and leptin resistance. J. Biol. Chem. *274*, 30059–30065. https://doi.org/10.1074/jbc.274.42.30059.

26. Chappell, P.E., White, R.S., and Mellon, P.L. (2003). Circadian gene expression regulates pulsatile gonadotropin-releasing hormone (GnRH) secretory patterns in the hypothalamic GnRH-secreting GT1-7 cell line. J. Neurosci. *23*, 11202–11213. https://doi.org/10.1523/jneurosci.23-35-11202.2003.

27. Klebe, R.J. (1969). Neuroblastoma : Cell culture analysis of a differentiating stem cell system. J. Cell Biol. *43*, 69A.

28. Dodd, G.T., Xirouchaki, C.E., Eramo, M., Mitchell, C.A., Andrews, Z.B., Henry, B.A., Cowley, M.A., and Tiganis, T. (2019). Intranasal Targeting of Hypothalamic PTP1B and TCPTP Reinstates Leptin and Insulin Sensitivity and Promotes Weight Loss in Obesity. Cell Rep. *28*, 2905–2922.e5. https://doi.org/10.1016/j.celrep.2019.08.019.

29. Andersen, H.S., Olsen, O.H., Iversen, L.F., Sørensen, A.L.P., Mortensen, S.B., Christensen, M.S., Branner, S., Hansen, T.K., Lau, J.F., Jeppesen, L., et al. (2002). Discovery and SAR of a novel selective and orally

bioavailable nonpeptide classical competitive inhibitor class of protein-tyrosine phosphatase 1B. J. Med. Chem. *45*, 4443–4459. https://doi.org/10.1021/jm0209026.

30. Qin, Z., Pandey, N.R., Zhou, X., Stewart, C.A., Hari, A., Huang, H., Stewart, A.F.R., Brunel, J.M., and Chen, H.-H. (2015). Functional properties of Claramine: A novel PTP1B inhibitor and insulin-mimetic compound. Biochem. Biophys. Res. Commun. *458*, 21–27. https://doi.org/10.1016/j.bbrc.2015.01.040.

31. Howlett, A.C., and Fleming, R.M. (1984). Cannabinoid inhibition of adenylate cyclase. Pharmacology of the response in neuroblastoma cell membranes. Mol. Pharmacol. *26*, 532–538.

32. Nogueras-Ortiz, C., and Yudowski, G.A. (2016). The Multiple Waves of Cannabinoid 1 Receptor Signaling. Mol. Pharmacol. *90*, 620–626. https://doi.org/10.1124/mol.116.104539.

33. Gyombolai, P., Boros, E., Hunyady, L., and Turu, G. (2013). Differential beta-arrestin2 requirements for constitutive and agonist-induced internalization of the CB1 cannabinoid receptor. Mol. Cell. Endocrinol. *372*, 116–127. https://doi.org/10.1016/j.mce.2013.03.013.

34. Mo, W., Zhang, L., Yang, G., Zhai, J., Hu, Z., Chen, Y., Chen, X., Hui, L., Huang, R., and Hu, G. (2008). Nuclear beta-arrestin1 functions as a scaffold for the dephosphorylation of STAT1 and moderates the antiviral activity of IFN-gamma. Mol. Cell. *31*, 695–707. https://doi.org/10.1016/j.molcel.2008.06.017.

35. Ruiz de Azua, I., and Lutz, B. (2019). Multiple endocannabinoid-mediated mechanisms in the regulation of energy homeostasis in brain and peripheral tissues. Cell. Mol. Life Sci. *76*, 1341–1363. https://doi.org/10.1007/s00018-018-2994-6.

36. Katona, I., and Freund, T.F. (2012). Multiple functions of endocannabinoid signaling in the brain. Annu. Rev. Neurosci. *35*, 529–558. https://doi.org/10.1146/annurev-neuro-062111-150420.

37. El-Haschimi, K., Pierroz, D.D., Hileman, S.M., Bjørbaek, C., and Flier, J.S. (2000). Two defects contribute to hypothalamic leptin resistance in mice with diet-induced obesity. J. Clin. Invest. *105*, 1827–1832. https://doi.org/10.1172/jci9842.

38. Kievit, P., Howard, J.K., Badman, M.K., Balthasar, N., Coppari, R., Mori, H., Lee, C.E., Elmquist, J.K., Yoshimura, A., and Flier, J.S. (2006). Enhanced leptin sensitivity and improved glucose homeostasis in mice lacking suppressor of cytokine signaling-3 in POMC-expressing cells. Cell Metabol. *4*, 123–132. https://doi.org/10.1016/j.cmet.2006.06.010.

39. Thibault, K., Carrel, D., Bonnard, D., Gallatz, K., Simon, A., Biard, M., Pezet, S., Palkovits, M., and Lenkei, Z. (2013). Activation-Dependent Subcellular Distribution Patterns of CB1 Cannabinoid Receptors in the Rat Forebrain. Cerebr. Cortex *23*, 2581–2591. https://doi.org/10.1093/cercor/bhs240.

40. Bosier, B., Bellocchio, L., Metna-Laurent, M., Soria-Gomez, E., Matias, I., Hebert-Chatelain, E., Cannich, A., Maitre, M., Leste-Lasserre, T., Cardinal, P., et al. (2013). Astroglial CB1 cannabinoid receptors regulate leptin signaling in mouse brain astrocytes. Mol. Metabol. *2*, 393–404. https://doi.org/10.1016/j.molmet.2013.08.001.

41. Pranada, A.L., Metz, S., Herrmann, A., Heinrich, P.C., and Müller-Newen, G. (2004). Real time analysis of STAT3 nucleocytoplasmic shuttling. J. Biol. Chem. *279*, 15114–15123. https://doi.org/10.1074/jbc.M312530200.

42. Zhang, Z.Y., Dodd, G.T., and Tiganis, T. (2015). Protein Tyrosine Phosphatases in Hypothalamic Insulin and Leptin Signaling. Trends Pharmacol. Sci. *36*, 661–674. https://doi.org/10.1016/j.tips.2015.07.003.

43. Loh, K., Fukushima, A., Zhang, X., Galic, S., Briggs, D., Enriori, P.J., Simonds, S., Wiede, F., Reichenbach, A., Hauser, C., et al. (2011). Elevated Hypothalamic TCPTP in Obesity Contributes to Cellular Leptin Resistance. Cell Metabol. *14*, 684–699. https://doi.org/10.1016/j.cmet.2011.09.011.

44. Zabolotny, J.M., Bence-Hanulec, K.K., Stricker-Krongrad, A., Haj, F., Wang, Y., Minokoshi, Y., Kim, Y.B., Elmquist, J.K., Tartaglia, L.A., Kahn, B.B., and Neel, B.G. (2002). PTP1B regulates leptin signal transduction in vivo. Dev. Cell *2*, 489–495. https://doi.org/10.1016/s1534-5807(02)00148-x.

45. He, J.C., Gomes, I., Nguyen, T., Jayaram, G., Ram, P.T., Devi, L.A., and Iyengar, R. (2005). The G alpha(o/i)-coupled cannabinoid receptor-mediated neurite outgrowth involves Rap regulation of Src and Stat3. J. Biol. Chem. *280*, 33426–33434. https://doi.org/10.1074/jbc.M502812200.

46. Delgado-Peraza, F., Ahn, K.H., Nogueras-Ortiz, C., Mungrue, I.N., Mackie, K., Kendall, D.A., and Yudowski, G.A. (2016). Mechanisms of Biased beta-Arrestin-Mediated Signaling Downstream from the Cannabinoid 1 Receptor. Mol. Pharmacol. *89*, 618–629. https://doi.org/10.1124/mol.115.103176.

47. Srivastava, A., Gupta, B., Gupta, C., and Shukla, A.K. (2015). Emerging Functional Divergence of β-Arrestin Isoforms in GPCR Function. Trends Endocrinol. Metabol. *26*, 628–642. https://doi.org/10.1016/j.tem.2015.09.001.

48. Wess, J. (2022). The Two β-Arrestins Regulate Distinct Metabolic Processes: Studies with Novel Mutant Mouse Models. Int. J. Mol. Sci. *23*, 495. https://doi.org/10.3390/ijms23010495.

49. Liu, Z., Iyer, M.R., Godlewski, G., Jourdan, T., Liu, J., Coffey, N.J., Zawatsky, C.N., Puhl, H.L., Wess, J., Meister, J., et al. (2021). Functional Selectivity of a Biased Cannabinoid-1 Receptor (CB1R) Antagonist. ACS Pharmacol. Transl. Sci. *4*, 1175–1187. https://doi.org/10.1021/acsptsci.1c00048.

50. Tan, S., Liu, H., Ke, B., Jiang, J., and Wu, B. (2020). The peripheral CB(1) receptor antagonist JD5037 attenuates liver fibrosis via a CB(1) receptor/β-arrestin1/Akt pathway. Br. J. Pharmacol. *177*, 2830–2847. https://doi.org/10.1111/bph.15010.

51. Pydi, S.P., Cui, Z., He, Z., Barella, L.F., Pham, J., Cui, Y., Oberlin, D.J., Egritag, H.E., Urs, N., Gavrilova, O., et al. (2020). Beneficial metabolic role of β-arrestin-1 expressed by AgRP neurons. Sci. Adv. *6*, eaaz1341. https://doi.org/10.1126/sciadv.aaz1341.

52. Sun, J.J., Yang, H.T., Niu, G.J., Feng, X.W., Lan, J.F., Zhao, X.F., and Wang, J.X. (2016). β-Arrestin 1's Interaction with TC45 Attenuates Stat signaling by dephosphorylating Stat to inhibit antimicrobial peptide expression. Sci. Rep. *6*, 35808. https://doi.org/10.1038/srep35808.

53. Pelzel, C., Begitt, A., Wenta, N., and Vinkemeier, U. (2013). Evidence against a role for β-arrestin1 in STAT1 dephosphorylation and the inhibition of interferon-γ signaling. Mol. Cell. *50*, 149–156. https://doi.org/10.1016/j.molcel.2013.02.024.

54. Kang, J., Shi, Y., Xiang, B., Qu, B., Su, W., Zhu, M., Zhang, M., Bao, G., Wang, F., Zhang, X., et al. (2005). A nuclear function of beta-arrestin1 in GPCR signaling: regulation of histone acetylation and gene transcription. Cell *123*, 833–847. https://doi.org/10.1016/j.cell.2005.09.011.

55. Wakahara, R., Kunimoto, H., Tanino, K., Kojima, H., Inoue, A., Shintaku, H., and Nakajima, K. (2012). Phospho-Ser727 of STAT3 regulates STAT3 activity by enhancing dephosphorylation of phospho-Tyr705 largely through TC45. Gene Cell. *17*, 132–145. https://doi.org/10.1111/j.1365-2443.2011.01575.x.

56. Morello, G., Imperatore, R., Palomba, L., Finelli, C., Labruna, G., Pasanisi, F., Sacchetti, L., Buono, L., Piscitelli, F., Orlando, P., et al. (2016). Orexin-A represses satiety-inducing POMC neurons and contributes to obesity via stimulation of endocannabinoid signaling. Proc. Natl. Acad. Sci. USA *113*, 4759–4764. https://doi.org/10.1073/pnas.1521304113.

57. Drori, A., Gammal, A., Azar, S., Hinden, L., Hadar, R., Wesley, D., Nemirovski, A., Szanda, G., Salton, M., Tirosh, B., and Tam, J. (2020). CB1R regulates soluble leptin receptor levels via CHOP, contributing to hepatic leptin resistance. Elife *9*, e60771. https://doi.org/10.7554/eLife.60771.

58. Després, J.P., Golay, A., and Sjöström, L.; Rimonabant in Obesity-Lipids Study Group (2005). Effects of rimonabant on metabolic risk factors in overweight patients with dyslipidemia. N. Engl. J. Med. *353*, 2121–2134. https://doi.org/10.1056/NEJMoa044537.

59. Kirkham, T.C., Williams, C.M., Fezza, F., and Di Marzo, V. (2002). Endocannabinoid levels in rat limbic forebrain and hypothalamus in relation to fasting, feeding and satiation: stimulation of eating by 2-arachidonoyl glycerol. Br. J. Pharmacol. *136*, 550–557. https://doi.org/10.1038/sj.bjp.0704767.

60. Dodd, G.T., Andrews, Z.B., Simonds, S.E., Michael, N.J., DeVeer, M., Brüning, J.C., Spanswick, D., Cowley, M.A., and Tiganis, T.

(2017). A Hypothalamic Phosphatase Switch Coordinates Energy Expenditure with Feeding. Cell Metabol. *26*, 375–393.e7. https://doi.org/10.1016/j.cmet.2017.07.013.

61. Acharya, K.D., Nettles, S.A., Sellers, K.J., Im, D.D., Harling, M., Pattanayak, C., Vardar-Ulu, D., Lichti, C.F., Huang, S., Edwards, D.P., et al. (2017). The Progestin Receptor Interactome in the Female Mouse Hypothalamus: Interactions with Synaptic Proteins Are Isoform Specific and Ligand Dependent. eneuro *4*. https://doi.org/10.1523/eneuro.0272-17.2017.

62. González-García, I., García-Clavé, E., Cebrian-Serrano, A., Le Thuc, O., Contreras, R.E., Xu, Y., Gruber, T., Schriever, S.C., Legutko, B., Lintelmann, J., et al. (2023). Estradiol regulates leptin sensitivity to control feeding via hypothalamic Cited1. Cell Metabol. *35*, 438–455.e437. https://doi.org/10.1016/j.cmet.2023.02.004.

63. Conner, D.A., Mathier, M.A., Mortensen, R.M., Christe, M., Vatner, S.F., Seidman, C.E., and Seidman, J.G. (1997). beta-Arrestin1 knockout mice appear normal but demonstrate altered cardiac responses to beta-adrenergic stimulation. Circ. Res. *81*, 1021–1026. https://doi.org/10.1161/01.res.81.6.1021.

64. Zimmer, A., Zimmer, A.M., Hohmann, A.G., Herkenham, M., and Bonner, T.I. (1999). Increased mortality, hypoactivity, and hypoalgesia in cannabinoid CB1 receptor knockout mice. Proc. Natl. Acad. Sci. USA *96*, 5780–5785.

65. Tam, J., Vemuri, V.K., Liu, J., Bátkai, S., Mukhopadhyay, B., Godlewski, G., Osei-Hyiaman, D., Ohnuma, S., Ambudkar, S.V., Pickel, J., et al. (2010). Peripheral CB1 cannabinoid receptor blockade improves cardiometabolic risk in mouse models of obesity. J. Clin. Invest. *120*, 2953–2966. https://doi.org/10.1172/JCI42551.

66. Godlewski, G., Jourdan, T., Szanda, G., Tam, J., Cinar, R., Harvey-White, J., Liu, J., Mukhopadhyay, B., Pacher, P., Ming Mo, F., et al. (2015). Mice lacking GPR3 receptors display late-onset obese phenotype due to impaired thermogenic function in brown adipose tissue. Sci. Rep. *5*, 14953. https://doi.org/10.1038/srep14953.

67. O'Hayre, M., Eichel, K., Avino, S., Zhao, X., Steffen, D.J., Feng, X., Kawakami, K., Aoki, J., Messer, K., Sunahara, R., et al. (2017). Genetic evidence that β-arrestins are dispensable for the initiation of β(2)-adrenergic receptor signaling to ERK. Sci. Signal. *10*, eaal3395. https://doi.org/10.1126/scisignal.aal3395.

68. Biener, E., Charlier, M., Ramanujan, V.K., Daniel, N., Eisenberg, A., Bjørbaek, C., Herman, B., Gertler, A., and Djiane, J. (2005). Quantitative FRET imaging of leptin receptor oligomerization kinetics in single cells. Biol. Cell (Paris) *97*, 905–919. https://doi.org/10.1042/bc20040511.

69. Kozak, M. (1987). An analysis of 5'-noncoding sequences from 699 vertebrate messenger RNAs. Nucleic Acids Res. *15*, 8125–8148. https://doi.org/10.1093/nar/15.20.8125.

70. Horváth, V.B., Soltész-Katona, E., Wisniewski, É., Rajki, A., Halász, E., Enyedi, B., Hunyady, L., Tóth, A.D., and Szanda, G. (2021). Optimization of the Heterologous Expression of the Cannabinoid Type-1 (CB1) Receptor. Front. Endocrinol. *12*, 740913. https://doi.org/10.3389/fendo.2021.740913.

71. Erdélyi, L.S., Balla, A., Patócs, A., Tóth, M., Várnai, P., and Hunyady, L. (2014). Altered agonist sensitivity of a mutant v2 receptor suggests a novel therapeutic strategy for nephrogenic diabetes insipidus. Mol. Endocrinol. *28*, 634–643. https://doi.org/10.1210/me.2013-1424.

72. Klarenbeek, J.B., Goedhart, J., Hink, M.A., Gadella, T.W.J., and Jalink, K. (2011). A mTurquoise-based cAMP sensor for both FLIM and ratiometric read-out has improved dynamic range. PLoS One *6*, e19170. https://doi.org/10.1371/journal.pone.0019170.

73. Buehler, E., Chen, Y.C., and Martin, S. (2012). C911: A bench-level control for sequence specific siRNA off-target effects. PLoS One *7*, e51942. https://doi.org/10.1371/journal.pone.0051942.

74. Jourdan, T., Nicoloro, S.M., Zhou, Z., Shen, Y., Liu, J., Coffey, N.J., Cinar, R., Godlewski, G., Gao, B., Aouadi, M., et al. (2017). Decreasing CB(1) receptor signaling in Kupffer cells improves insulin sensitivity in obese mice. Mol. Metabol. *6*, 1517–1528. https://doi.org/10.1016/j.molmet.2017.08.011.

75. Mukhopadhyay, B., Cinar, R., Yin, S., Liu, J., Tam, J., Godlewski, G., Harvey-White, J., Mordi, I., Cravatt, B.F., Lotersztajn, S., et al. (2011). Hyperactivation of anandamide synthesis and regulation of cell-cycle progression via cannabinoid type 1 (CB_1) receptors in the regenerating liver. Proc. Natl. Acad. Sci. USA *108*, 6323–6328. https://doi.org/10.1073/pnas.1017689108.

76. Gyombolai, P., Tóth, A.D., Tímár, D., Turu, G., and Hunyady, L. (2015). Mutations in the 'DRY' motif of the CB1 cannabinoid receptor result in biased receptor variants. J. Mol. Endocrinol. *54*, 75–89. https://doi.org/10.1530/jme-14-0219.

STAR★METHODS

KEY RESOURCES TABLE

REAGENT or RESOURCE	SOURCE	IDENTIFIER
Antibodies		
α-CB_1R	Immunogenes, Hungary	RRID:AB_2813823
α-pSTAT3 (tyrosine)	Cell Signaling Technology	Cat#9145; RRID:AB_2491009
α-pSTAT3 (serine), monoclonal	Cell Signaling Technology	Cat#9136; RRID:AB_331755
α-pSTAT3 (serine), polyclonal	Cell Signaling Technology	Cat#9134; RRID:AB_331589
α-STAT3	Cell Signaling Technology	Cat#4904; RRID:AB_331269
α-βarrestin-1	Cell Signaling Technology	Cat#30036; RRID:AB_2798985
α-βarrestin-2	Cell Signaling Technology	Cat#3857; RRID:AB_2258681
α-TC PTP	Cell Signaling Technology	Cat#58935; RRID:AB_2799550
α-PTP 1B	Cell Signaling Technology	Cat#5311; RRID:AB_10695100
α-GFP	Cell Signaling Technology	Cat#2956; RRID:AB_1196615
Chemicals, peptides, and recombinant proteins		
ACEA	Tocris	Cat#1319
recombinant murine leptin	Research And Diagnostic Systems	Cat# 498-OB
recombinant human leptin	Research And Diagnostic Systems	Cat#398-LP
Critical commercial assays		
mouse/rat specific leptin ELISA kit	B-Bridge International	Cat#K1006-1
ultra-sensitive mouse leptin ELISA kit	Crystal Chem Inc.	Cat#90080
GFP-Trap magnetic agarose	Chromotek	Cat#gtma-20
Experimental models: Cell lines		
Neuro 2a cells	American Type Culture Collection (ATCC)	CCL-131
HEK 293 cells	American Type Culture Collection (ATCC)	CRL-1573
$\beta arr1^{-/-}/\beta arr2^{-/-}$ HEK 293 cells	Wakahara et al.[15]	
GT1-7 cell	produced by P.L. Mellon and colleagues, described, *e.g.*, in[26]	
Experimental models: Organisms/strains		
C57Bl/6J mice	The Jackson Laboratory	JAX stock Cat#000664; RRID:IMSR_JAX:000664
C57Bl/6J $CB_1R^{-/-}$ mice	produced and described by Zimmer et al.[64]	
C57Bl/6J $\beta arr1^{-/-}$ mice (B6.129X1(Cg)-$Arrb1^{tm1Jse}$/J)	produced and described by Conner et al.[63]	JAX stock Cat#011131; RRID:IMSR_JAX:011131
Oligonucleotides (for control design see Buehler et al.[72])		
mus musculus cnr1 siRNA; GCAUCAAGAGCACUGUUAA(UU)	Horváth et al.[70]	N/A
mus musculus βarrestin1 (arrb1) siRNA; GGGACUUUGUGGACCACAU(UU)	this paper	N/A
mus musculus βarrestin2 (arrb2) siRNA; ACGUCCAUGUCACCAACAA(UU)	Gyombolai et al.[76]	N/A

(*Continued on next page*)

Continued

REAGENT or RESOURCE	SOURCE	IDENTIFIER
mus musculus TC PTP (PTPN2) siRNA 1; GCUCUUAUCUGAAGAUGUA(UU)	this paper	N/A
mus musculus TC PTP (PTPN2) siRNA 2; CGGUGGAAAGAACUUUCUA(UU)	this paper	N/A
mus musculus PTP 1B (PTPN1) siRNA; GUCGCGAAGCUUCCUAAGA(UU)	this paper	N/A
Recombinant DNA		
homo sapiens TK-CB_1R	Horváth et al.[70]	N/A
homo sapiens TK-Δ64-CB_1R	Horváth et al.[70]	N/A
mus musculus ObR_b-CFP	Biener et al.[68]	N/A
Rluc-EPAC-eYFP (cAMP sensor)	original Klarenbeek et al.,[71] modified Erdélyi et al.[72]	N/A
Software and algorithms		
Multi-wavelength translocation module	Molecular Devices	ImageXpress Micro Confocal High-Content Imaging System
Deposited data		
Raw and analyzed data, western blots, IHC images	this paper, Mendeley data	https://doi.org/10.17632/53jfh7rd2b.1

RESOURCE AVAILABILITY

Lead contact

Further information and requests for resources and reagents should be directed to and will be fulfilled by the lead contact, Gergo Szanda (szanda.gergo@med.semmelweis-univ.hu).

Materials availability

This study did not generate new unique reagents.

Data and code availability

- The data reported in this paper were deposited Mendeley Data: https://doi.org/10.17632/53jfh7rd2b.1. Non-deposited or additional raw data will be shared by the lead contact upon request.
- This article does not report original code.
- Any additional information required to reanalyze the data reported in this paper is available from the lead contact upon reasonable request.

EXPERIMENTAL MODEL AND STUDY PARTICIPANT DETAILS

Ethics statement and animal experiments

All animal procedures were approved by the Institutional Animal Care and Use Committee of NIAAA, NIH; experiments were performed according to conventional guidelines. C57Bl/6J WT and β-arrestin1 knock out animals[63] were from The Jackson Laboratory (Bar Harbor, ME, USA; stock #011131). C57Bl/6J $CB_1R^{-/-}$ mice[64] and wild-type littermates were generated as previously described.[65] In order to acclimate, all animals were housed for at least 14 days in the institutional animal facility and were switched to single housing at least 7 days prior to experimentation. Mice had free access to water and were fed a standard rodent diet (NIH-31 rodent diet) *ad libitum* while maintained on a 12:12 light/dark cycle (17:30-5:30 or 18:30-6:30 depending on daylight saving time) at an ambient temperature of 21 ± 1°C and at a relative humidity of 62-68%. Animals were habituated to handling prior to performing experiments. Core body temperature and ambulatory activity were monitored as described earlier.[66] Only male animals between 12-16 weeks of age were investigated (in this range, age did not affect results, data were pooled.)

In all experiments, animals were fasted overnight as follows: 15 min before the onset of the dark period mice were place in a new cage together with some bedding and nestlet from the old cage to carry over own scent, and a new nestlet was also provided to aid nesting and enrich environment. Mice had free access to water during the dark cycle, food was not present. At the exact beginning of the light period, body weights were measured, and animals were assigned into treatment groups in a randomized manner while keeping average body weight even among groups. Then, drugs were prepared and experiments started 60 min after the onset of the light period (adding up to a total of 13 h food deprivation at the beginning of experiments).

In experiments with exogenous leptin treatment, mice were first treated with ACEA (10 or 2 mg/kg; *i.p.*) or vehicle (90% sterile isotonic NaCl + 5% sterile DMSO + 5% Tween 80) at 0 min (~13h after the start of food deprivation) and then with leptin (0.3 mg/kg, *i.p.*) or saline 30 or 45 min later. Samples were collected 45 or 60 min after the leptin injection. In the fasting – re-feeding paradigm, body weights were measured at the exact beginning of the light period and re-feeding (if any) started 60 min later (again, adding up to a total of 13 h food deprivation in the refed groups). Food was made available *ad libitum* (in the refed group only) for 2 or 4 hours (data were pooled) and after this refeeding period all mice were placed in a new cage without food. At this point, animals were injected with the CB_1R agonist ACEA (2 or 10 μM, *i.p.*) or with vehicle (90% sterile isotonic NaCl + 5% sterile DMSO + 5% Tween 80). Samples were collected 45 or 90 min after the injection (data were pooled). In all experiments, mice were anesthetised with isoflurane at the nominal end of the incubation period (except for when CSF was collected or PFA perfusion followed, see below), and blood was collected from the retrobulbar sinus. Then, animals, still under anaesthesia, were euthanized by decapitation. Hypothalami and CSF were obtained as described in pertinent sections below.

Cell culture, transfection and cell stimulation

GT1-7 cells[26] (kindly provided by Dr. Pamela L. Mellon, University of California), Neuro-2a (ATCC), and β-arrestin1/2 double knock-out HEK 293 cells[67] were cultured in Dulbecco's Modified Eagle Medium (DMEM) containing 10% foetal bovine serum and supplemented with 100 U/ml penicillin and 100 μg/ml streptomycin ("complete DMEM"). (DMEM formulations with 1.5 g/L $NaHCO_3$ were used exclusively in order to attain pH 7.4 at 5% CO_2 and 37°C.)

GT1-7 cells were plated into 6-well plates at a density of 6.5×10^5/well on day 1. Transfection of plasmid DNA or siRNA was performed on day 2 (overnight) in Ultra-MEM with Lipofectamine-2000 (0.2 μL/cm^2). Neuro-2a cells were plated on day 1 onto poly-L-lysine coated 6-well plates, poly-L-lysine coated 96-well plates or onto poly-L-lysine coated iBidi μ-slides at a density of $2.5\text{-}3\times10^5$/well or $4\text{-}7\times10^3$/well (iBidi μ-slides). Transfection of siRNA into Neuro-2a cells was performed as follows: on day 2, cells were treated with siRNA in Ultra-MEM for 6 h in the presence of Lipofectamine RNAiMAX (0.5 μL/cm^2). Then, on day 3, cells were again treated with siRNA in complete DMEM for 6 h with Lipofectamine RNAiMax. DNA transfection (if any) was performed overnight (day 2 to 3) in complete DMEM with Lipofectamine LTX + Plus Reagent (0.6 μL/cm^2 Lipofectamine LTX + 0.5 μL/μg total DNA Plus Reagent). Unless otherwise indicated, siRNA concentration was 30 nM and construct DNA amount was 0.025-0.2 μg/cm^2/construct.

Cells were serum deprived by changing the complete medium to empty DMEM on day 3 (overnight serum starvation) or day 4 (8-10 h serum starvation) before stimulation on day 4. One h prior to experiments, medium was changed to DMEM + 10 mM HEPES (pH 7.4) + 3.94 mM HCO_3^- (incubation solution) and cell stimulation was carried out also in this incubation medium in order to minimize pH changes during experiments. In order to maintain osmolality, isosmotic stock solutions of HEPES (193 mM HEPES + 107 mM NaOH) and HCO_3^- (154 mM $NaHCO_3$) were used. At the end of the incubation period, cells were rinsed with ice-cold PBS twice and lysed in lysis buffer (for immunoblotting, *v.i.*) or in Trizol reagent (for RT qPCR, *v.i.*). In some experiments, 6-well plates were snap frozen with liquid nitrogen and stored at -80°C until analysis.

For STAT3 translocation assay, β-arrestin1/2 double KO HEK 293 cells were plated onto 24-well No.1.5 polymer coverslip bottomed plates at 0.75×10^5/well and transfected with 1.5 μl/well Lipofectamine 2000.

Passage numbers 4–30 were used. At all steps, bicarbonate-buffered media were equilibrated at 37°C and 5% CO_2 for at least 12 h before application to avoid thermal and pH stress to cells.

METHOD DETAILS

For further details on materials see Tables S1–S3.

Materials, pharmacons and formulations

All chemicals were obtained from Sigma Aldrich (St. Louis, MO, USA), unless specified otherwise. CB_1R agonists, CB_1R antagonists, URB 597 and TCS 401 were purchased from Tocris (Bristol, UK). Recombinant leptin was purchased from Research and Diagnostic (R&D) Systems, dissolved in sterile 20 mM Tris-HCl (pH 8.0) and stored at -80°C in small aliquots. For intraperitoneal injection, leptin was diluted in isotonic sterile PBS or isotonic sterile NaCl to a concentration of 0.03 mg/mL. ACEA and URB 597 were diluted in a mixture of 90% sterile isotonic NaCl + 5% sterile DMSO + 5% Tween 80 to final concentrations of 0.2 mg/mL and 0.1 mg/mL, respectively. Injection volumes were limited to 10 μL/g of body weight.

If drugs were obtained in anhydrous ethanol, ethanol was first evaporated with N_2 and sterile dimethyl sulfoxide (DMSO) was then used for reconstitution. (DMSO was stored in small aliquots at -20°C to avoid water absorption into the solvent.) All stock solutions were split into small aliquots and a maximum of 2 freeze-thaw cycles were allowed. In cell culture experiments, final concentration of DMSO was limited to 0.15%.

Constructs, siRNA

The CFP-tagged long isoform of the murine leptin receptor (mLEPR-CFP or $mObR_b$-CFP; kindly provided by Dr. Arieh Gertler (The Hebrew University of Jerusalem)) was constructed by ligating mLEPR to CFP and then inserting into pECFP-N1 plasmid backbone using AgeI and BsrGI restriction sites, as described previously.[68] Human ObR_b was C-terminally fused to 3 tandem myc tags and subcloned into the pCMV3 vector wherein a Kozak consensus sequence (GCCACC[69]) was introduced 5′ to the start codon. Murine STAT3 was C-terminally fused to a tandem of cyan and yellow fluorescent proteins (CFP and YFP, respectively) by subcloning the murine STAT3 insert into a pSVLΔEcoRI vector (including the sequence for the CFP-YFP tag) using XhoI and BstEII, restriction sites, as described.[41] (STAT3-CFP-YFP was generously provided by Dr. Gerhard Müller-Newen, University Hospital Aachen.) In most experiments, human STAT3-eGFP, expressed in the pEGFP-N1 vector, was used. Human and murine wild-type CB_1R and Δ64-CB_1R (lacking the N-terminal 1-64 amino acids) were expressed in pcDNA3.1 vectors (driven by the early-immediate CMV promoter for high-level expression). Unless otherwise stated, the thymidine kinase promoter driven human Δ64-CB_1R was used as this construct was extensively characterized by our group and was found to closely mimic the behaviour of endogenous WT CB_1Rs.[70] For fluorescent labelling, human WT and human Δ64-CB_1R were inserted into mVenus-N1 expression vectors. *Renilla* luciferase labelled β-arrestin1 and β-arrestin2 constructs were expressed in a pCMV based vector backbone coding for the human codon optimizes *Renilla* luciferase and were designed by inserting rat β-arrestin1 and β-arrestin2 sequences, respectively, 5′ to the *Renilla* luciferase sequence.[33] Cytoplasmic cAMP concentration was monitored with an EPAC-based intramolecular BRET cAMP sensor constructed by Erdélyi *at al.*[71] based on the sensor of Klarenbeek and co-workers.[72] For dsRNA sequences also see Table S2. Control (non-silencing) dsRNA sequences were designed according to the "C9-11" method.[73] Mouse β-arrestin2 siRNA and mouse CB_1R siRNA sequences were previously published.[33,74] Working concentrations of dsRNAs were 10-30 nM.

Western blotting

Hypothalamic brain samples were homogenized in 300 or 400 μL complete lysis buffer (*v.i.*) at 4°C in a Precellys-24 tissue homogenizer with ceramic beads (Bertin Technologies, France) whereas cultured neuronal cells were suspended in 4°C complete lysis buffer (*v.i.*) using a volume of 150-200 μL/9.5 cm^2 growth area. After a 30 min incubation period on wet ice, insoluble material was removed by centrifugation at ~20.000 g (4°C for 10 min) and total protein concentration of the supernatant was determined with BCA Assay (Thermo Fisher Scientific). The complete lysis buffer was based on a modified RIPA buffer containing: 150 mM NaCl, 1% Triton X-100, 1% sodium deoxycholate, 0.1% SDS, 1 mM EDTA, 1 mM EGTA and 20 mM Tris-HCl (pH 7.35 at 4°C). This modified RIPA buffer was supplemented with either cOmplete Protease Inhibitor Cocktail and PhosSTOP phosphatase inhibitor tablets (Roche) or with 1:100 Aprotinin, 1 mM sodium orthovanadate, 1 mM phenylmethylsulfonyl fluoride, 1:100 protease inhibitor cocktail, 1:100 phosphatase inhibitor cocktail 1 and 1:100 phosphatase inhibitor cocktail 2. After the addition of 4x Laemmli sample buffer (Bio-Rad) protein extracts were separated in reducing mini or midi format Tris-glycine polyacrylamide gradient gels (4-15%, Bio-Rad). Final concentration of β-mercaptoethanol in the samples was set to 5%; no heat-denaturation was applied. Proteins

were then blotted onto nitrocellulose membranes using the Transblot-cell semi-dry transfer system with the appropriate transfer packs (Bio-Rad). Some samples were separated by electrophoresis in Bis-Tris-HCl polyacrylamide gradient gels (4-15%) and in MOPS running buffer (Bio-Rad) and were blotted onto nitrocellulose membrane using traditional "wet" transfer (50V for 9 h).

Membranes were blocked with Tris buffered saline + 0.1% Tween-20 (TBST) supplemented with 5% milk and incubated with primary antibodies in TBST + 0.1% sodium azide overnight at 4°C. Horseradish peroxidase conjugated secondary antibodies (PerkinElmer) were applied in TBST + 5% milk at room temperature for 1 h and luminescence was captured using either X-ray films (Fujifilm), Syngene G:BOX (Syngene, Frederick, MD, USA) or Azure 600 (Azure Biosystems, Dublin, CA, USA) chemiluminescence imaging systems. West Pico Plus (ThermoFisher) or custom-made substrate solution (100 mM Tris-Cl, 1.1 mM luminol, 0.2 mM p-coumaric acid, 2.6 mM H_2O_2, pH 8.5) were used for detection. Captured images were processed by the brightness/contrast and background subtraction modules of Image J (NIH) and by Adobe Illustrator to align blots. (For the complete list of antibodies see Table S3.) The integrated density of individual protein bands was measured on raw images with the Image J software and the ratio of phosphorylated to total protein (p/t ratio) was regarded as degree of activation. Unless otherwise specified, data were normalized to the average of the leptin-only or leptin + vehicle treated group.

Measurement of plasma and CSF leptin concentration

For the simultaneous measurement of plasma leptin levels and hypothalamic STAT3 activation, mice were anesthetised with isoflurane and blood (~ 0.5 mL) was collected from the retrobulbar sinus. Anesthetised animals were then euthanized by decapitation and the mediobasal hypothalamus was quickly removed and snap frozen in liquid nitrogen for immunoblot, lipid or transcriptional analysis. Serum leptin levels were determined using a mouse/rat specific leptin ELISA kit (B-Bridge International) according to the kit's protocol.

CSF was collected as described earlier.[15] Briefly, 5 min before the end of the nominal incubation period, mice were anesthetized with isoflurane. Under a dissection microscope a dorsal midline incision was made rostral of the nuchal crest to the mid-cervical region and subcutaneous tissue and muscles were separated by blunt dissection until the dura mater was exposed. Then a pre-made sterile glass capillary pipette was used to penetrate into the cisterna magna and collect CSF (~ 5 μL). Blood (~ 0.5 mL) was then obtained from the retrobulbar sinus and animals, still under isoflurane anaesthesia, were euthanized by decapitation. The brain was removed and the approx. 0.5 mm thick section of the mediobasal hypothalamus was removed and snap frozen in liquid nitrogen for further analysis. CSF leptin concentrations were determined with the Ultra-Sensitive Mouse Leptin ELISA kit (Crystal Chem Inc.) according to the manufacturer's protocol.

STAT3 translocation assay

Fluorescent-labelled STAT3 plasmids (*v. Constructs*) were transfected into Neuro-2a cells as described in *Cell culture and transfection*. At the end of the incubation period, cells were fixed with either ice-cold 4% PFA-PBS or with -20°C 100% methanol for 15 min at room temperature. Wells were then washed 5x with PBS and were filled with PBS + 0.1% sodium azide + 0.5 or 1 μM Hoechst 33342 (Invitrogen) and kept in this solution until and during microscopic assessment. Images of nuclei (Hoechst, excitation at 360-390 nm, emission between 420-470 nm) and STAT3 (excitation at 460-490 nm, emission between 516-555 nm) were acquired with the ImageXpress Micro Confocal High-Content Imaging System (Molecular Devices, San Jose, CA, USA) in wide field (Nikon Plan Fluor ELWD 20x/0.45NA objective) or in spinning wheel confocal mode (Nikon Super Plan Fluor ELWD 40x/0.6NA objective, 2x binning). Nuclear and perinuclear (also referred to as non-nuclear cytosolic) regions were separated with the multi-wavelength translocation assay within the MetaXpress module (Molecular Devices). Hoechst 33342 positive areas were demarcated where pixel intensity exceeded the local background by ~ 1.5-fold and where the following shape descriptors applied: maximal diameter 30 μm, minimal diameter 6 μm. The edge of each Hoechst 33342^+ area was regarded as apparent nuclear membrane; pixels within the Hoechst 33342^+ area and located at least 1.8 μm from the apparent nuclear membrane were considered as the nuclear region. The cytosolic (perinuclear) region was defined as a 0.6 μm wide area laying 0.5 μm outside the apparent nuclear membrane and enclosing the nucleus entirely (Figure S2A). The ratio of average STAT3 fluorescence within the nuclear region (nF) to the average fluorescence intensity or to the integrated density of STAT3 in the perinuclear cytosolic region (cF and cD, respectively) were used as measure of STAT3 nuclear (trans)location. (Evaluating nF/cF or nF/cD provided practically identical results.) Cells were analyzed only if STAT3 nF was at least 3-fold higher than that measured in

non-transfected cells (cellular background). β-arrestin nuclear translocation was assessed along same analytical steps. Unless otherwise stated, data were normalized to the average of the vehicle-only or, in case of dose-response curves, to that of the lowest leptin concentration treated group.

Lipid measurements

Hypothalami were snap frozen in liquid N_2 and tissue concentration of endocannabinoids was measured by stable isotope dilution liquid chromatography/tandem mass spectrometry (LC-MS/MS) following the exact protocol described earlier.[75]

Immunohistochemistry

For immunohistochemical analysis, 10 min prior to the end of the nominal incubation period, mice were anesthetized with ketamine-xylazine (100 mg/kg and 20 mg/kg *i.p.*, respectively) and perfused trans-cardially with 15 ml ice-cold PBS and then with 20 ml 4% paraformaldehyde in PBS (PFA-PBS, pH 7.4). Brains were removed and post-fixed overnight in 4% PFA-PBS at 4°C. Coronal sections (40-50 μm) were cut with vibratome (Leica, Germany) and floating samples were collected in PBS. Antigen retrieval was carried out in 1% NaOH + 1% H_2O_2 in dH_2O for 40 min. Samples were then further treated with (in PBS) 0.1% Triton X-100 (45 min), 0.75% glycine (30 min; pH ∼ 7.2) and finally with 0.3% SDS for 10 min. Floating sections were washed 3x5 min in PBS between each treatment. Blocking was performed for 2 h in 0.3% Triton X-100 PBS + 5% serum from the species of the secondary antibody. Brain sections were then incubated with primary antibodies in the appropriate blocking solution at 4°C overnight. After a brief wash (2x5 min in PBS) coronal sections were stained with fluorescent-labelled secondary antibodies for 2 h in 3% BSA + 0.3% Triton X-100 in PBS. (For the complete list of antibodies see Table S3). Finally, sections were mounted onto glass microscope slides and covered with mounting medium with DAPI and cover glasses with low autofluorescence in the UV range. Fluorescent images were acquired with the LSM750 laser scanning confocal microscope system (Zeiss, Jena, Germany) or with the Nikon A1 laser scanning confocal microscope (Nikon, Minato, Tokyo, Japan) and images were processed and analyzed with the LSM Image Browser (Zeiss) and Image J software (NIH, Bethesda, MD, USA). All steps were carried out at room temperature unless otherwise specified.

BRET measurements of cytoplasmic cAMP and of β-arrestin – CB_1R interaction

BRET measurements were carried out as specified earlier.[76] Briefly, HEK 293 cells were transfected with 0.175 μg construct DNA (see *Constructs*) in suspension with 0.5 μl/well Lipofectamine 2000 (Invitrogen) according to the manufacturer's protocol. Cells were plated on white poly-L-lysine coated 96-well plates at 50.000 cells/well density. Neuro 2a cells were plated on 6-well plates at 500.000 cells/well density. The next day cells were transfected with 2 μg plasmid DNA using Lipofectamine LTX (Invitrogen). Measurements were performed 24-28h after transfection. After 3.5 h serum deprivation of HEK 293 cells in serum-free DMEM the solution was switched to modified Krebs-Ringer medium containing 120 mM NaCl, 4.7 mM KCl, 1.2 mM CaCl2, 0.7 mM MgSO4, 10 mM glucose, 10 mM Na-HEPES (pH 7.4). After 3 h serum deprivation, Neuro 2a cells were detached using PBS-EDTA, centrifuged for 4 min at 2.000 RPM, resuspended in modified Krebs-Ringer medium, and transferred to white 96-well plates. Measurements were started with the addition of 5 μM coelenterazine *h* (Regis Technologies) and luminescence was measured at 480 nm (luciferase) and 530 nm (YFP or mVenus) with a Thermo Scientific Varioskan Flash Reader (Thermo Scientific). BRET ratio was calculated by dividing emission intensities measured at 530 nm and 480 nm, or, in the case of cAMP measurement, 480 nm was divided by 530 nm (1/BRET ratio) so that cAMP increases are represented by a positive increment in the signal. BRET ratio values were normalized to baseline (i.e. before the addition of forskolin) and interpreted as changes in cytosolic [cAMP] ($\Delta[cAMP]_{cyto}$). For β-arrestin – CB_1R interaction measurements, baseline correction was applied for all data points, and BRET ratio of the vehicle treated group was subtracted from all data prior to normalization.

Real-time qPCR

For the isolation of RNA, hypothalamus samples were homogenized with Precellys-24 tissue homogenizer (Bertin Technologies, France) or, in case of adherent cells, were scraped in Trizol reagent (Invitrogen). RNA was isolated with RNeasy Lipid Tissue Mini Kit (Qiagen) and then treated with DNase I (Invitrogen) according to the manufacturers' protocols. RNA was reverse-transcribed into cDNA with the Iscript cDNA kit (Bio-Rad) and subsequent real-time qPCR was performed using the StepOne Plus real time PCR system with Fast SYBR Green master mix (Applied Biosystems). QuantiTect (Qiagen) primers were used for amplification (Table S2).

Co-immunoprecipitation

After stimulation, cells were lysed in an ice-cold buffer containing 150 mM NaCl, 10 mM Tris/HCl (pH 7.5), 0.5 mM EDTA and 0.5% Triton X-100 supplemented with 1:100 Aprotinin, 1 mM sodium orthovanadate, 1 mM phenylmethylsulfonyl fluoride, 1:100 protease inhibitor cocktail, 1:100 phosphatase inhibitor cocktail 1 and 1:100 phosphatase inhibitor cocktail 2. The insoluble material was removed by centrifugation (17.000x g for 10 min at 4°C) and then the GFP-tagged proteins were precipitated (1 h at 4°C) using Chromotek GFP-trap magnetic agarose according to the manufacturer's protocol. Eluates were subjected to SDS-PAGE and membranes were developed as described for Western blotting.

QUANTIFICATION AND STATISTICAL ANALYSIS

Data analysis and statistics

Means + s.e.m. or +/– s.e.m. are shown unless indicated otherwise. Data were obtained from at least 3 independent experiments or specified otherwise. In some experiments, in case high impact outliers were present, minimal and maximal values have been uniformly excluded in all groups using the trimmed mean approach or outliers were removed by the ROUT method. For bar graphs, number of observations are indicated in left to right (L to R) orientation in the legend to the figure; for high-throughput STAT3 translocation assay, the lowest and highest n numbers are specified (min-max). For calculating significance of differences, Student's unpaired t-test and Mann-Whitney test, one and two-way ANOVA and post-hoc tests were used, as appropriate. Dose-response curves were fitted using the 3-parametered log[agonist] – response equation ((Y=Bottom + (Top-Bottom)/(1+10(LogEC50-X))). In the high-throughput STAT-translocation experiments, number of observations was set to attain a power of approx. 0.9 ($\beta \approx 0.1$) at α=0.05. Data were analyzed with Microsoft Excel 2016, GraphPad Prism 5 and Statistica 13.